



THE PENNSYLVANIA
STATE UNIVERSITY

IONOSPHERIC RESEARCH

Scientific Report 433

DESIGN OF A SIMPLE GERDIEN CONDENSER FOR IONOSPHERIC D-REGION CHARGED PARTICLE DENSITY AND MOBILITY MEASUREMENTS

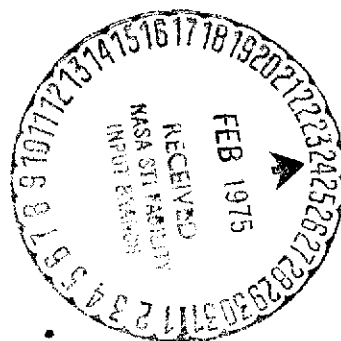
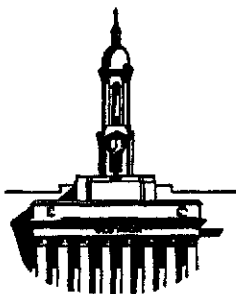
by

Hashem Farrokh

January 6, 1975

The research reported in this document was supported by The National Aeronautics and Space Administration under Grant No. NGR 39-009-218 and the U.S. Army Research Office under Grant DA-ARO-D-31-124-72-G158.

IONOSPHERE RESEARCH LABORATORY



University Park, Pennsylvania

NASA-CR-142107) DESIGN OF A SIMPLE GERDIEN
CONDENSER FOR IONOSPHERIC D-REGION CHARGED
PARTICLE DENSITY AND MOBILITY MEASUREMENTS
(Pennsylvania State Univ.) 75 P HC \$4.25
N75-17024
Unclas
CSC 04A G3/46 09916

DOCUMENT CONTROL DATA - R & D

(Security classification of title, body of abstract and indexing annotation must be entered when the overall report is classified)

1. ORIGINATING ACTIVITY (Corporate author)		2a. REPORT SECURITY CLASSIFICATION	
The Ionosphere Research Laboratory		2b. GROUP	
3. REPORT TITLE			
Design of a Simple Gerdien Condenser for Ionospheric D-Region Charged Particle Density and Mobility Measurements			
4. DESCRIPTIVE NOTES (Type of report and inclusive dates)			
Scientific Report			
5. AUTHOR(S) (First name, middle initial, last name)			
Hashem Farrokh			
6. REPORT DATE		7a. TOTAL NO. OF PAGES	7b. NO. OF REFS
January 6, 1975		65	
8a. CONTRACT OR GRANT NO.		9a. ORIGINATOR'S REPORT NUMBER(S)	
NGR 39-009-218		PSU-IRL-SCI-433	
b. PROJECT NO.		9b. OTHER REPORT NO(S) (Any other numbers that may be assigned this report)	
c.			
d.			
10. DISTRIBUTION STATEMENT			
Supporting Agencies			
11. SUPPLEMENTARY NOTES		12. SPONSORING MILITARY ACTIVITY	
		The National Aeronautics and Space Administration U.S. Army Research Office	
13. ABSTRACT			
<p>The theory of a Gerdien Condenser operating in a collision-controlled medium is reviewed. Design and electronics of a Gerdien condenser probe suitable for flying on the Arcas rocket is presented. Aerodynamics properties of the instrument in continuous flow are discussed. The method of data reduction and experimental results of one successful flight at White Sands Missile Range (WSMR), New Mexico on 11 January 1974 is reported. The result of this investigation shows: positive ions in two relatively distinct mobility groups between 47 and 65 km and a more continuous distribution of mobilities between 38 and 47 km.</p>			

PSU-IRL-SCI-433

Classification Numbers 1.5.1, 3.2.2

Scientific Report 433

Design of a Simple Gerdien Condenser for Ionospheric
D-Region Charged Particle Density and Mobility Measurements

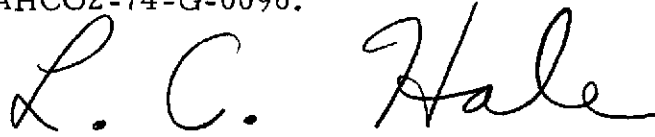
by

Hashem Farrokh

January 6, 1975

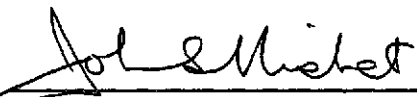
The research reported in this document was supported by The National Aeronautics and Space Administration under Grant Number NGR 39-009-218 and the U.S. Army Research Office under Grant Numbers DA-ARO-D-31-124-72-G158 and DAHCO2-74-G-0096.

Submitted by:



L. C. Hale
Professor of Electrical Engineering

Approved by:



J. S. Nisbet, Director
Ionosphere Research Laboratory

Ionosphere Research Laboratory

The Pennsylvania State University

University Park, Pennsylvania 16802

ACKNOWLEDGMENTS

The author wishes to express his appreciation to Dr. L. C. Hale for his guidance in this research.

The research in this document was supported by the National Aeronautics and Space Administration Grant No. NGR 39-009-218 and by the U.S. Army Research Office Grant No. DA-ARO-D-31-124-72-G158.

The field operation in which the Gerdien condenser was launched on January 11, 1974, was supported by supplementary ARO Grant No. DAHCO2-74-G-0096 with funds provided by Atmospheric Sciences Laboratory of White Sands Missile Range, who also supplied much gratefully acknowledged assistance.

TABLE OF CONTENTS

	Page
ACKNOWLEDGMENTS	ii
LIST OF FIGURES	iv
ABSTRACT	vii
I. INTRODUCTION	1
1.1 Importance of the Problem	1
1.2 Previous Related Research	2
II. THEORY	5
2.1 Ion Collection	5
2.2 The Current-Voltage Characteristic of the Gerdien Condenser	7
2.3 Space Charge Effect	10
2.4 Ion Mobility	12
2.5 Fringing Field Effect	18
2.6 Photo Emission Effect	18
III. DESIGN AND INSTRUMENTATION	20
3.1 Design of Simplified Version	20
3.2 Instrumentation	23
3.2.1 Sweep Voltage Generator	23
3.2.2 Electrometer	29
3.2.3 Voltage Controlled Oscillator (VCO)	29
3.2.4 Telemetry System	30
3.2.5 Power Supply	30

	Page
IV. AERODYNAMICS CONSIDERATIONS	31
4.1 Flow Regimes	31
4.2 Compressibility Effect	34
4.3 Velocity Distribution	38
V. FLIGHTS AND DATA	51
5.1 The Gerdien Condenser Launch	51
5.2 Reduction of Data	52
VI. CONCLUSIONS	61
REFERENCES	62
APPENDIX A: COMPUTER PROGRAM	65

LIST OF FIGURES

Figure		Page
1	Current-Voltage Characteristics of the Gerdien Condenser .	6
2	Variation of Electric Field of the Gerdien Condenser with Charge Density	13
3	Apparent Decrease of Ion Current as a Result of Fringing Field at the Condenser Entrance	19
4	Gerdien Condenser/Blunt Probe Assembly	21
5	Schematic of the Gerdien Condenser Assembly	22
6	Schematic of the Gerdien Condenser Instrumentation	24
7	Sweep Voltage Generator Circuit	25
8	Logarithmic Electrometer Circuit	26
9	Voltage Controlled Oscillator Circuit	27
10	Transmitter Circuit	28
11	Variation of Mean Free Path with Altitude	32
12	The Flow Regimes for the Gerdien Condenser	33
13	Descent Velocity as a Function of the Altitude	36
14	Variation of the Gerdien Condenser Reynolds Number with Altitude	37
15	Flow Conditions	39
16	Variation of $f(\chi)$ with χ	41
17	Variation of Flow Core-Length with Altitude	45
18	Entry Flow in a Circular Cylinder	46
19	Descent Velocity of the Gerdien Condenser and Calculated Velocity of Air Flow	50
20	Calibration Current as a Function of Frequency	53
21	The Gerdien Condenser Sweep Waveforms	54
22	Descent Time as a Function of Altitude	55

Figure		Page
23	Two Typical Current-Voltage Characteristics of the Gerdien Condenser	57
24	Positive Ion Density as a Function of Altitude	59
25	Positive Ion Mobility as a Function of Altitude	60

ABSTRACT

The theory of a Gerdien Condenser operating in a collision-controlled medium is reviewed. Design and electronics of a Gerdien condenser probe suitable for flying on the Arcas rocket is presented. Aerodynamics properties of the instrument in continuous flow are discussed. The method of data reduction and experimental results of one successful flight at White Sand Missile Range (WSMR), New Mexico on 11 January 1974 is reported. The result of this investigation shows: positive ions in two relatively distinct mobility groups between 47 and 65 km and a more continuous distribution of mobilities between 38 and 47 km.

CHAPTER I

INTRODUCTION

1.1 Importance of the Problem

The ionospheric D-region is located at about 60 to 90 kilometers (km) altitude and is largely responsible for the absorption of radio waves. Historically, the most important ionospheric measurements in this region have utilized remote probing with such waves (Deeks, 1966; Coyne and Belrose, 1972; Lee and Ferraro, 1969). However, in terms of the physical parameters of this region, these methods provide information only about free electrons, specifically density and collision frequency. The various remote sounding techniques are ineffective below about 65 km; and some of these methods have limitations in that they can only be used during disturbed conditions, when the electron concentration is high enough to give a reliable measurement (Thrane et al., 1968).

Direct measurements in this region may be made only by sounding rocket at present, since it is above the region where balloons can ascend and below the normal operational altitude of satellites. However, the shock waves generally characterized at sounding rockets may seriously affect direct measurements in this region (Hale et al., 1972). Some parachute borne measurements which avoid this problem have been performed, including the blunt probe.

The basic quantities measured by the blunt probe are the polar charged particle conductivities, σ^+ and σ^- , and in order to obtain ion density (N) the mobility (k) must be known (since $\sigma = Nek$). Heretofore,

positive ion mobility was assumed to be that appropriate for "small" molecular ions at a temperature and density determined as a function of altitude from an appropriate atmospheric model (CIRA). Recently, however; a large amount of evidence has accumulated that these values of mobility may not in fact be correct, and that a substantial number of ions may not be "small" ($\text{AMU} < 100$), but quite large and of very much lower mobility; a summary of this evidence has been given by Chesworth (1974). A direct measurement utilizing a subsonic Gerdien condenser "aspiration probe" was made by Rose and Widdel (1972) which indeed showed positive ions to have such small mobilities, as well as mobilities for the "small" ions larger than expected. However, all of this data was obtained from a single launch of the payload.

It can be concluded, therefore; that there is a need for more information about ionospheric mobility. The Gerdien condenser is one device that can be used to measure charged particle mobility. The angle of attack problem associated with earlier instruments (Pederson, 1964) can be largely eliminated by the use of the more aerodynamically stable decelerating devices which are available today.

1.2 Previous Related Research

The Gerdien condenser has been named after Gerdien (1905), who first demonstrated use of two concentric cylinders for ion collection at ground level. Some investigators have used this instrument to measure atmospheric ion conductivities and mobilities for many years. A review of their work has been given by Knoll et al. (1964). Further development of the Gerdien condenser as a mobility spectrometer have been reported (Israel and Schulz, 1933; Nolan and Kenny, 1952). Israel

and Schulz were able to differentiate four groups of ions and their seasonal and geographical variations by using these devices at sea level.

The Gerdien condenser has been used in numerous experiments to measure low altitude (up to about 30 km) atmospheric ion density and conductivity on balloon flights (Stergis et al., 1955; Woessner et al., 1958; Kroening, 1960). The results of these experiments may be subject to some serious errors (Paltridge, 1965). Some measurements have also been done using the instrument on aircraft (Sagalyn, 1958; Kraakevik, 1958). Due to aircraft noise there may be some uncertainties in this type of measurements.

Bourdeau, Whipple and Clark (1959) have described a rocket experiment using two Gerdien condensers mounted on the nosetip of a Viking rocket. Their measurements show an ion conductivity less than they expected. The authors have pointed out the uncertainty in their measurement, since the shock waves may disturb the air flow through condenser as the rocket is moving with a supersonic velocity ($M = 4$). The shock waves may also cause thermal ionization and alter the composition of the medium. Whipple (1964) has described further development of Gerdien condenser systems mounted at the tip of a rocket nosecone, and some of measurement results from Aerobee experiment at Fort Churchill, Canada, has been reported by Whipple (1964).

Pederson (1964) has employed a parachute-borne Gerdien condenser technique to measure ionospheric ion densities. In addition to the angle of attack problem, the wake of the detached rocket nosecone in front of the probe complicates the air flow through the condenser in Pederson's experiment.

Perhaps the most reliable ionospheric charged particle measurement using the parachute-borne Gerdien condenser to date was by Rose and Widdel (1972). In addition to their analyzer system which has a second aspiration system behind it to remove all charged particles from the air stream (keeping the charge neutrality at the end of the sonde), a flowmeter similar (in size and geometry) to the condenser was used to determine the velocity of the air stream through the aspiration condenser. They have also pointed out that nickel coating of the system eliminates a surface effect present with aluminum which caused a zero shift in the current-voltage characteristic, and by using care in aerodynamical design their system is relatively unaffected to an angle of attack up to 20° to 25° . Their experimental results on May 15, 1968 from Perdasdefogu, Sardina shows: two groups of positive ions in the height region 58 to 72 km, one group of positive ion below about 52 km, and no data in the altitude range of 52 to 58 km. Their data shows only one group of negative ion which have a mobility about the same as the mobility of lighter group of positive ions.

More recently Conley (1974), after a review of Gerdien condenser theory, has presented the experimental results of D-region positive ion density and mobility measurements during a PCA event. In four experiments which took place at Churchill Research Range (CRR), the Gerdien condenser was mounted on a black Brant rocket having a supersonic speed ($M = 3$ to 4). Conley's data shows one group of positive ions with mobility slightly less than the lighter ions (between about 58 and 72 km) and mixed ion (below 52 km), measured by Rose and Widdel (1972). However, the data indicate no low mobility group of ions, which may be due to the supersonic nature of the experiment; the shock wave may prevent the sampling of these ions.

CHAPTER II

THEORY

2.1 Ion Collection

The Gerdien condenser consists basically of two concentric cylinders, Figure 1.a, positioned so that air flows through the instrument at sufficiently low potential difference between the inner and outer cylinders; ions are collected at a rate proportional to the flow rate and this potential difference.

Before saturation, the general equation for positive ion collection can be written as:

$$J = -eD\nabla N^+ + kN^+e\nabla V + N^+eS \quad (2.1)$$

where J is current density; D is coefficient of diffusion of positive ion; k is mobility of positive ion, N^+ is number density of positive ion; V is potential; e is electrostatic charge; and S is the convection velocity.

The first term in equation (2.1) is due to diffusion. The second term represents the contribution of conduction, and the third term is due to convection. In the classical operation of the condenser, it is usually assumed that air flow is parallel to the axis of the instrument. Under this condition the convection term can be neglected and equation (2.1) reduces to:

$$J = -eD\nabla N^+ + kN^+e\nabla V \quad (2.2)$$

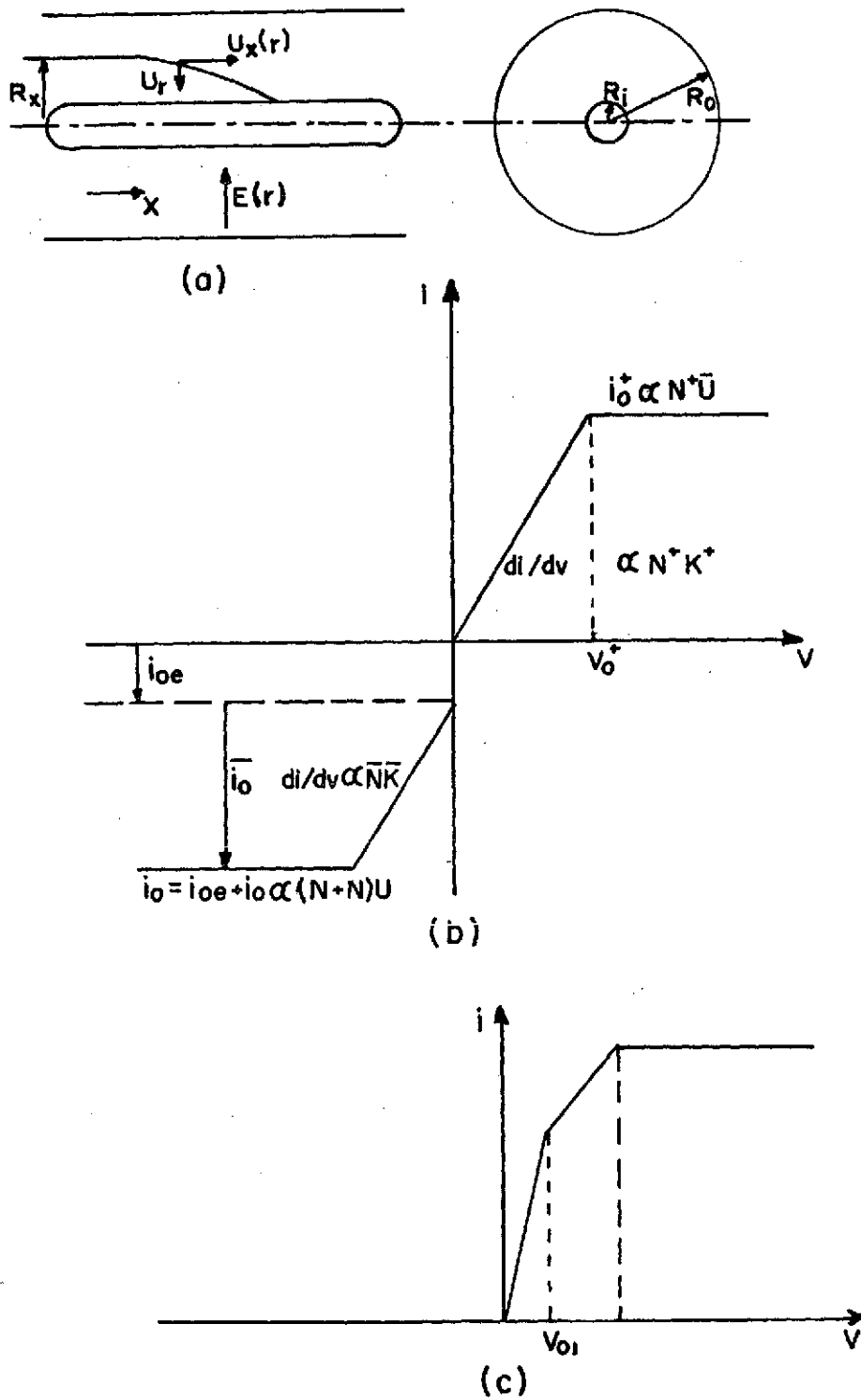


Figure 1. Current-Voltage Characteristics of the Gerdien Condenser.

Under the assumption that ∇N^+ has a value at most of the same order of ∇V , the first term in equation (2.2) can be neglected compared to the second term. This can be shown using Einstein's relation:

$$\frac{D}{k} = \frac{KT}{e} \quad (2.3)$$

where K is the Boltzmann constant and T is the temperature in degrees Kelvin.

In upper atmosphere the value of $\frac{KT}{e} \leq .03V$, therefore, for a probe potential much greater than this equation (2.2) becomes simply:

$$J = kN^+e\nabla V \quad (2.4)$$

It has been shown (Hoult, 1965; Sonin, 1967) that the equation of the form (2.4) is applicable to a wide class of probes operating in a continuous medium.

2.2 The Current-Voltage Characteristic of the Gerdien Condenser

Consider the Gerdien condenser shown in Figure 1.a consisting of two concentric cylinders of radii R_0 and R_1 . An electric field is set up between the two cylinders in such a manner that the ions to be measured drift toward the central electrode which is the collector in this arrangement. In order to obtain the current-voltage characteristic of the Gerdien condenser, the trajectory of a positive ion, entering the condenser at a radius R_x , would be considered (Pederson, 1964). The radial drift velocity U_r is:

$$U_r = k^+E(r) \quad (2.5)$$

where $E(r)$ is the radial electric field and is given by:

$$E(r) = -\frac{V}{r} \frac{1}{\ln \frac{R_o}{R_i}} \quad (2.6)$$

where r is any radial distance from condenser axis. The volume rate of air flow through the cross-section $\pi(R_x^2 - r^2)$ is:

$$\phi_r^x = \int_r^{R_x} U_x(r) 2\pi r dr \quad (2.7)$$

where $U_x(r)$ is air stream velocity and is a function of x and r (Paltridge, 1965). In a time increment dt , the following relation holds:

$$dt = \frac{dr}{U_r} = \frac{dx}{U_x(r)}$$

$$dx = \frac{U_x(r)}{U_r} dr$$

substituting the value of U_r from equation (2.5), dx integrates to:

$$x = \int_{R_x}^r \frac{U_x(r)}{k^+ E(r)} dr = \frac{-\ln \frac{R_o}{R_i}}{k^+ V} \int_{R_x}^r U_x(r) r dr \quad (2.8)$$

combining equations (2.7) and (2.8):

$$x = \frac{1}{2\pi} \frac{\ln \frac{R_o}{R_i}}{V} \phi_r^x \quad (2.9)$$

If a positive ion enters the condenser at a radius R_{x1} , a voltage V_1 is necessary to obtain $x = L$, at the end of the central electrode, when $r = R_i$. All ions entering the condenser at a radius of less than

R_{x1} are collected by the central electrode resulting in a current of:

$$i_1 = N^+ e \phi_{R_1}^{R_{x1}} = N^+ e \frac{C}{\epsilon} k^+ V_1 \quad (2.10)$$

where ϵ is the permittivity of the medium and $C = \frac{2\pi\epsilon L}{\ln \frac{R_o}{R_i}}$ is the capacity of condenser.

It can be seen from equation (2.10) that before saturation, the current is proportion to a voltage V_1 , $\frac{\partial i_1}{\partial V_1}$ is proportion to the conductivity $\sigma^+ = eN^+k^+$. The saturation current is given by:

$$i_o^+ = N^+ e \phi_{R_i}^{R_o} = N^+ e \frac{C}{\epsilon} k^+ V_o \quad (2.11)$$

If instead of $U_x(r)$ an average velocity \bar{U} be assumed, then using equations (2.8) and (2.11) the saturation voltage can be written as:

$$V_o = \frac{\epsilon \phi_{R_i}^{R_o}}{Ck^+} = \frac{\epsilon \pi (R_o^2 - R_i^2)}{C} \frac{\bar{U}}{k^+} \quad (2.12)$$

The equations (2.11) and (2.12) are unchanged if the electric field is reversed and the outer cylinder becomes the collector. They are also valid for negative ions provided that N^+ and k^+ are replaced by N^- and k^- , respectively. The current voltage characteristic of the Gerdien condenser is shown in Figure 1.b. One type of positive ion and one type of negative ion and electron have been assumed to be present in the air aspirated through the condenser. The negative saturation current i_o^- is proportional to $\bar{U} (N^- + N)$ where N is the electron density. Electrons having a high mobility are collected for very small voltages as shown in the figure. Stray fields at two ends of the condenser have been neglected.

The current-voltage characteristics of the Gerdien condenser when there are different types of ions of different densities and mobilities can be obtained by superposition. Under this condition equations (2.10) and (2.11) become:

$$i = e \frac{C}{\epsilon} V \sum_n^n k_n N_n \quad (2.13)$$

$$i_o = e \frac{C}{\epsilon} V_o \sum_n^n k_n N_n \quad (2.14)$$

Figure 1.c shows the ideal current-voltage characteristic of a Gerdien condenser, if two types of positive ions are present. The saturation current i_o is proportional to $(N_1^+ + N_2^+) \bar{U}$. The derivative of the current-voltage characteristic is proportional to $(N_1^+ K_1^+ + N_2^+ K_2^+)$ for $V < V_{o1}$ and proportional to $N_2 K_2$ for $V_{o1} < V < V_{o2}$.

From the foregoing discussion, it is evident that the ion conductivity, $N^+ e K^+$, can be deduced from the slope of the current-voltage characteristic, and $N^+ \bar{U}$ can be derived from the saturation current. In order to obtain information about K^+ either N^+ or \bar{U} must be known. The Gerdien condenser can be operated as a mobility spectrometer as demonstrated in Figure 1.c. It is, however, necessary to have an accurate current-voltage characteristics if ions of different mobilities are to be distinguished.

2.3 Space Charge Effect

The relation for electric field in the last section (equation 2.6) is a solution of Laplace's equation which assumes the existence of space charge neutrality in the Gerdien condenser. If ions of one polarity are collected more quickly than the other polarity, a space

charge will be present between two electrodes of the Gerdien condenser. This space charge may distort the electric field in the condenser. An estimate of the space charge can be made by solving the Poisson's equation assuming one type of particle remains constant through the condenser. Poisson's equation for a Gerdien condenser can be written as:

$$\frac{d^2V}{dr^2} + \frac{1}{r} \frac{dV}{dr} = - \frac{N^+e}{\epsilon} \quad (2.15)$$

whose general solution for constant positive charge density is:

$$E(r) = \frac{dV}{dr} = - \frac{N^+er}{4\epsilon} + \frac{B}{r} \quad (2.16)$$

and

$$V = - \frac{N^+er^2}{4\epsilon} + B \ln r + C \quad (2.17)$$

where B and C are the constants of integration and are evaluated by applying the boundary conditions at $r = R_i$, $V = 0$; and at $r = R_o$, $V = V_o$:

$$B = \frac{V_o}{\ln \frac{R_o}{R_i}} + \frac{N^+e}{4\epsilon} \frac{R_o^2 - R_i^2}{\ln \frac{R_o}{R_i}} \quad (2.18)$$

$$C = - B \ln R_i + N^+e \frac{R_i^2}{4\epsilon} \quad (2.19)$$

Substituting equations (2.18) and (2.19) for B and C, equations (2.16) and (2.17) become:

$$E(r) = \frac{V_o}{r \ln \frac{R_o}{R_i}} - \frac{N^+e}{2\epsilon} \left[r - R_o^2 - \frac{R_i^2}{2 r \ln \frac{R_o}{R_i}} \right] \quad (2.20)$$

$$V = \frac{V_o \ln \frac{r}{R_i}}{\ln \frac{R_o}{R_i}} + \frac{N^+ e}{4\epsilon} (R_o^2 - R_i^2) \left[\frac{\ln \frac{r}{R_i}}{\ln \frac{R_o}{R_i}} - (r^2 - R_i^2) \right] \quad (2.21)$$

The distribution of electric field for positive charge densities of $N^+ = 10^5 \text{ cm}^{-3}$, $N^+ = 10^4 \text{ cm}^{-3}$ and $N^+ = 0$ with applied potential of $V = 5\text{v}$ and $V = 10\text{v}$ is shown in Figure 2. It is shown that for charge densities of the order up to 10^4 cm^{-3} , the space charge neutrality assumption causes no significant error. However, above 80 km, it is believed that electron and positive ions are the dominant charge particles. Electrons having a high mobility, are picked up by the collector at the opening of Gerdien condenser. Positive ions follow the air stream through the condenser, where they represent a space charge (density 10^5 cm^{-3} or more) in the condenser. Therefore, when Gerdien condenser is used above 80 km the effect of space charge must be taken into the account.

2.4 Ion Mobility

When a mixture of ions and gas are under the influence of an electric field they gain energy from the field. If the energy acquired in one mean free path is small compared to thermal energy:

$$\left(\frac{M}{m} + \frac{m}{M} \right) eE\lambda \ll KT \quad (2.22)$$

where M is the mass of the gas molecule

m is the mass of the ions

λ is the mean free path

and after substitution inequality (2.22) becomes:

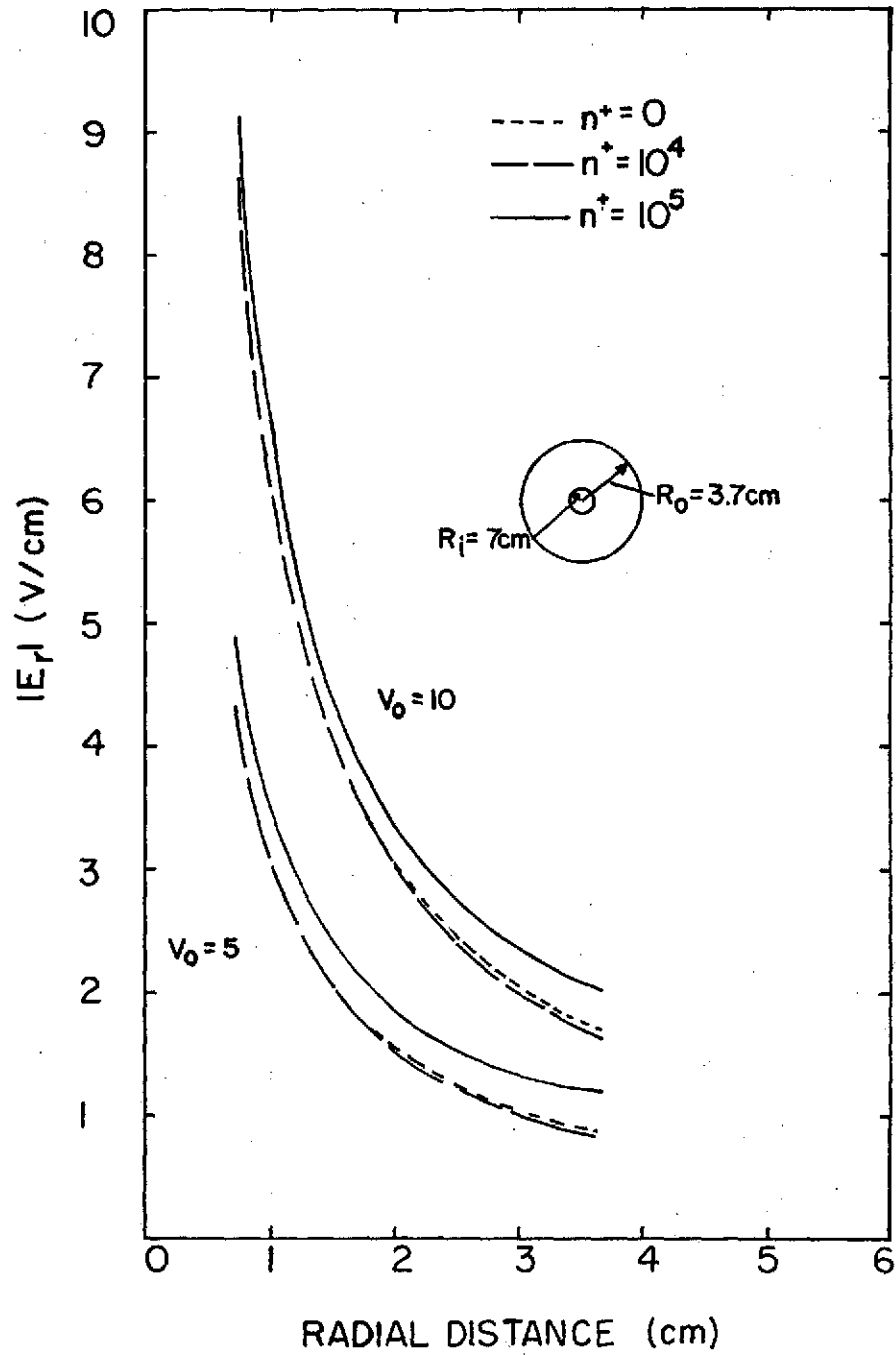


Figure 2. Variation of Electric Field of the Gerdien Condenser with Charge Density.

$$\left(\frac{M}{m} + \frac{m}{M}\right) eE \ll P\sigma \quad (2.23)$$

where P is the gas pressure and σ the collision cross section. If there is not too much difference between the masses of ions and molecules, inequality (2.23) reduces to:

$$\frac{E}{P} \ll 2 \frac{\sigma}{e} \approx 2 \frac{4\pi \times 10^{-16}}{5 \times 10^{-10}} \text{ e.s.u.}$$

or on in commonly employed units:

$$\frac{E}{P} \ll 2 \frac{\text{volts}}{\text{cm (mm Hg)}} \quad (2.24)$$

This is called low field case. For high field the limit becomes:

$$\frac{E}{P} \gg 2 \frac{\text{volts}}{\text{cm (mmHg)}} \quad (2.25)$$

The cases in which limit (2.24) holds the mobility of ions are independent of electric field so that the drift velocity:

$$U_d = kE$$

To calculate the drift velocity, it is considered that during the time between collision, t_λ , the ions move a distance d in the field and experience a force $F = eE$ and an acceleration $a = \frac{eE}{m}$, therefore:

$$d = \frac{1}{2} a t_\lambda^2 = \frac{eE}{2m} t_\lambda^2$$

and:

$$U_d = \frac{d}{t_\lambda} = \frac{1}{2} \frac{eE}{m} t_\lambda = \frac{Ee\lambda}{2m\bar{c}}$$

where \bar{c} is given as:

$$\frac{1}{c} = \left(\frac{8KT}{\pi m} \right)^{\frac{1}{2}}$$

thus, the mobility becomes:

$$k = \left(\frac{e}{2m} \right) \frac{\lambda}{c} \quad (2.26)$$

Equation (2.26) is a very simple expression for mobility, and neglects such effects as role of the mass of the parent gas, and forces between ion and gas molecules. There have been numerous theories to correct these deficiencies. A thorough discussion can be found in Loeb (1955). Langevin derived an expression, based on kinetic theory, for mobility as:

$$k = 0.815 \frac{e\lambda}{Mc} \sqrt{\frac{m+M}{m}} \quad (2.27)$$

where c is the root-mean-square-velocity of the gas molecules.

A more general treatment which also include high field cases was given by Wannier (1953). He assumes that collision cross section is velocity dependence and has the form:

$$\sigma(U)U^{\alpha} = \Gamma \quad (2.28)$$

where α and Γ are constants. This assumption has two important special cases which arise, taking $\alpha = 0$ and $\alpha = 1$. The case of $\alpha = 0$ is that of a constant mean free path representing solid elastic impact. The case of $\alpha = 1$ is that of a constant mean free time and is applicable to the polarization force. Based on the above assumption, using the Boltzmann equation he shows that for low electric field the mean drift velocity can be written as:

$$U_d = \text{const} \left(\frac{a}{N\Gamma} \right)^{\frac{1}{2-\alpha}} \quad (2.29)$$

where N is the number density of molecules. This gives the variation of the drift velocity with the field E .

For constant mean free path, $\alpha = 0$ ($\Gamma = \sigma$) and equation (2.27) reduces to:

$$\langle U_d \rangle = \text{const} a^{\frac{1}{2}} \lambda^{\frac{1}{2}} = \text{const} \left(\frac{eE}{m} \lambda \right)^{\frac{1}{2}} \quad (2.30)$$

where the drift velocity is proportion to \sqrt{E} and mobility proportional to $\frac{1}{\sqrt{E}}$. For constant mean free time, $\alpha = 1$ ($\Gamma = \sigma U$):

$$\langle U_d \rangle = \text{const} a\tau = \text{const} \frac{eE}{m} \tau \quad (2.31)$$

where the drift velocity is proportional to E and mobility is constant.

Note that in deriving equation (2.30) and (2.31), the quantities

$\lambda = \frac{1}{N\sigma}$ and $\tau = \frac{1}{N\sigma U}$ have been considered.

For high electric field, the mean drift velocity is given by Wannier as:

$$\langle U_d \rangle = \text{const} \frac{eE}{mN\Gamma} \left(\frac{KT}{M} \right)^{\frac{\alpha-1}{2}} \quad (2.32)$$

with the special cases:

$$\langle U_d \rangle = \text{const} a \lambda \left(\frac{KT}{M} \right)^{-\frac{1}{2}} = \text{const} \frac{eE}{M} \lambda \left(\frac{KT}{M} \right)^{-\frac{1}{2}} \quad (2.33)$$

for constant mean free path $\alpha = 0$; and:

$$\langle U_d \rangle = \text{const} \text{ a } \tau = \text{const} \frac{eE}{m} \tau$$

for constant mean free time of $\alpha = 1$.

As shown in the above discussion for $\alpha = 0$ in both high and low electric fields the drift velocity is proportional to $E^{\frac{1}{2}}$ and mobility proportional to $E^{-\frac{1}{2}}$. When $\alpha = 1$ in both cases, the drift velocity is proportional to E and mobility is constant.

Wannier's theory has been successful in interpreting the mobility data for many cases. At low applied field the mobility is constant. This can be explained as a constant mean free time between ion and molecular collisions. Quite frequently, mobility is constant even when the limit (2.25) prevails. The region where mobility depends on $\frac{E}{P}$ varies with ion and gases, it probably depends on the strength of forces acting between ions and molecules. At still higher field the mobility is proportional to $E^{-\frac{1}{2}}$ consistent with a constant mean free path between ion and molecular collisions.

For the Gerdien condenser under the investigation $\frac{E}{P} > 2V\text{cm}^{-1} (\text{mm Hg})^{-1}$ for an applied potential of 1 volt at altitudes greater than 52 km. As shown in Figure 2 the electric field for a given potential varies within the condenser. It is clear, therefore; that $\frac{E}{P}$ varies from low to high field within the instrument. However, the fact that the applied sweep potential changes the electric field from low to high field is not important. The important fact is that the mobility (the slope of current-voltage characteristic curve) in the condenser remains constant.

2.5 Fringing Field Effect

The electric field strength and configuration at the front opening of the condenser have a controlling effect on incoming ions or electrons. The collecting area of the condenser depends on these stray fields. It has been shown (Schmeer et al., 1962) that for large positive bias voltages the saturation current, instead of remaining constant, actually falls as shown in Figure 3. This happens because lines of force originating from the surface of outer cylinder have a repelling effect on arriving positive ions.

It has been suggested (Jespersen et al., 1968) that for reducing this effect both ends of the condenser may be closed by a wire mesh. By doing so, the field lines will not extend outside the wire mesh. Rose and Widdel (1972), however, have reported this reduces the collection efficiency of the instrument considerably (more than 50 percent).

2.6 Photo Emission Effect

Photo-electrons will be released from metal surface of the probe when it is irradiated by solar ultraviolet light and solar x-rays (Pederson, 1964). If sunlight hits the collector of the condenser some of the electrons released may be drawn out of the condenser by the air flow. This may give rise to a spurious output current, which sometimes may be comparable to actual ion current. Shielding can prevent this photo emission effect. Photo emission, however, can provide the effect of a low impedance connection between an exposed electrode and ambient medium.

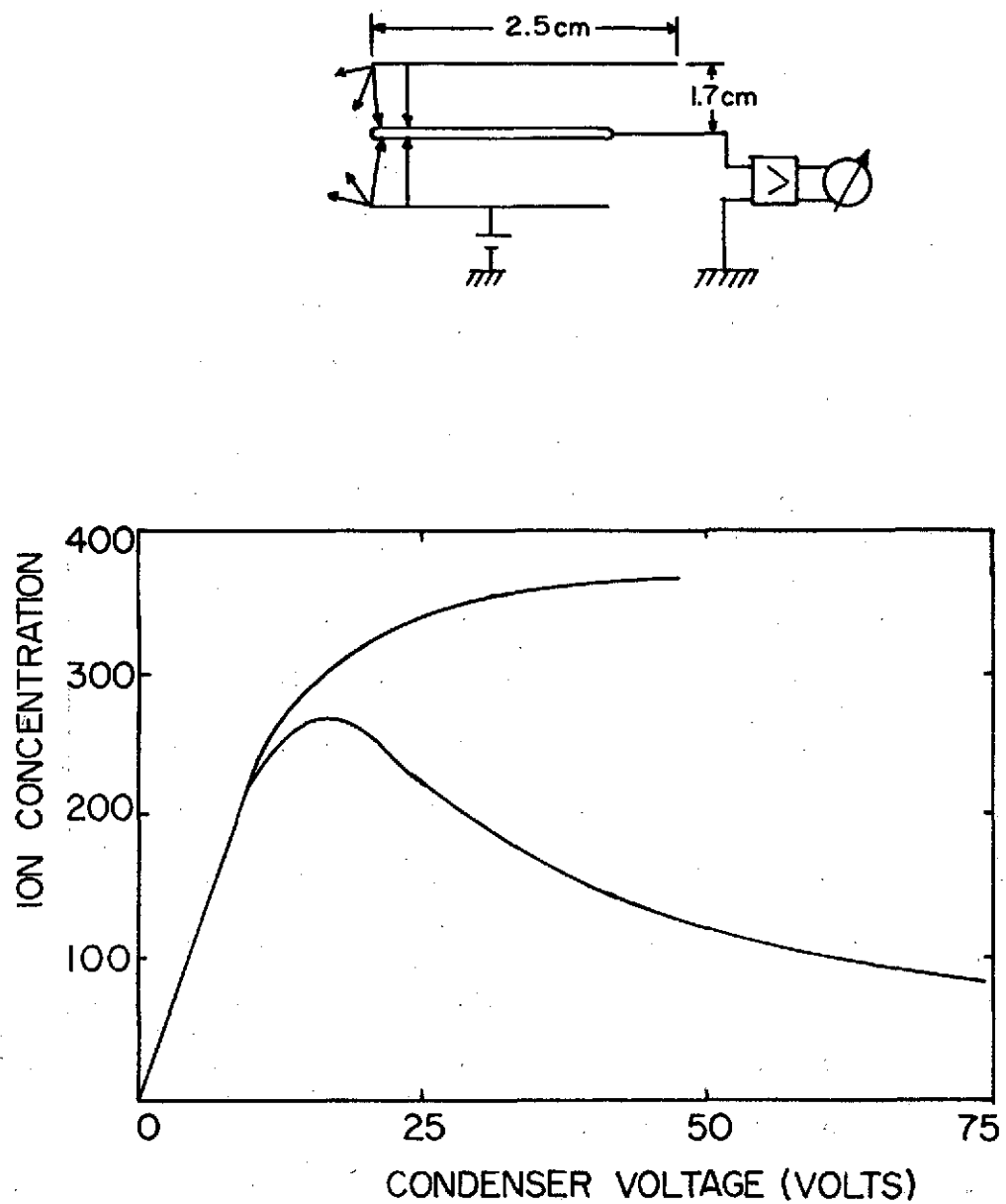


Figure 3. Apparent Decrease of Ion Current as a Result of Fringing Field at the Condenser Entrance (after Schmeer et al., 1962.

CHAPTER III

DESIGN AND INSTRUMENTATION

3.1 Design of Simplified Version

A picture of the complete probe is shown in Figure 4. It consists basically of two parts:

- (a) An aspiration condenser to measure the ionospheric charge particles concentration and their respective mobilities.
- (b) A "blunt probe" assembly which is used to provide the various parts of the electronics and telemetry system.

A schematic cross-section of the whole system is shown in Figure 5. The Gerdien condenser is made from two concentric aluminum cylinders. The outer cylinder is 10.16 cm long and has a diameter of 7.4 cm and is held to the blunt probe by three supporting posts. The inner electrode (collector) has a length of half the outer cylinder (5.08 cm) and a diameter of 1.4 cm; it is positioned by the center post. This reduction in length will prevent the direct sunlight on the collector, therefore, it will reduce photo-emission effects. In addition, it reduces the fringing effect at the front aperture. Three side posts and the center post are electrically isolated with teflon insulation from the outer and inner electrodes, (see Figure 5) and they have the same potential as the guard ring of the blunt probe. The outer cylinder which is used as the driving electrode is electrically connected to the return electrode of the blunt probe. The collector is connected to the electrometer and has the same potential as the collector disc of the blunt probe, therefore, the supporting posts and guard ring are basically of

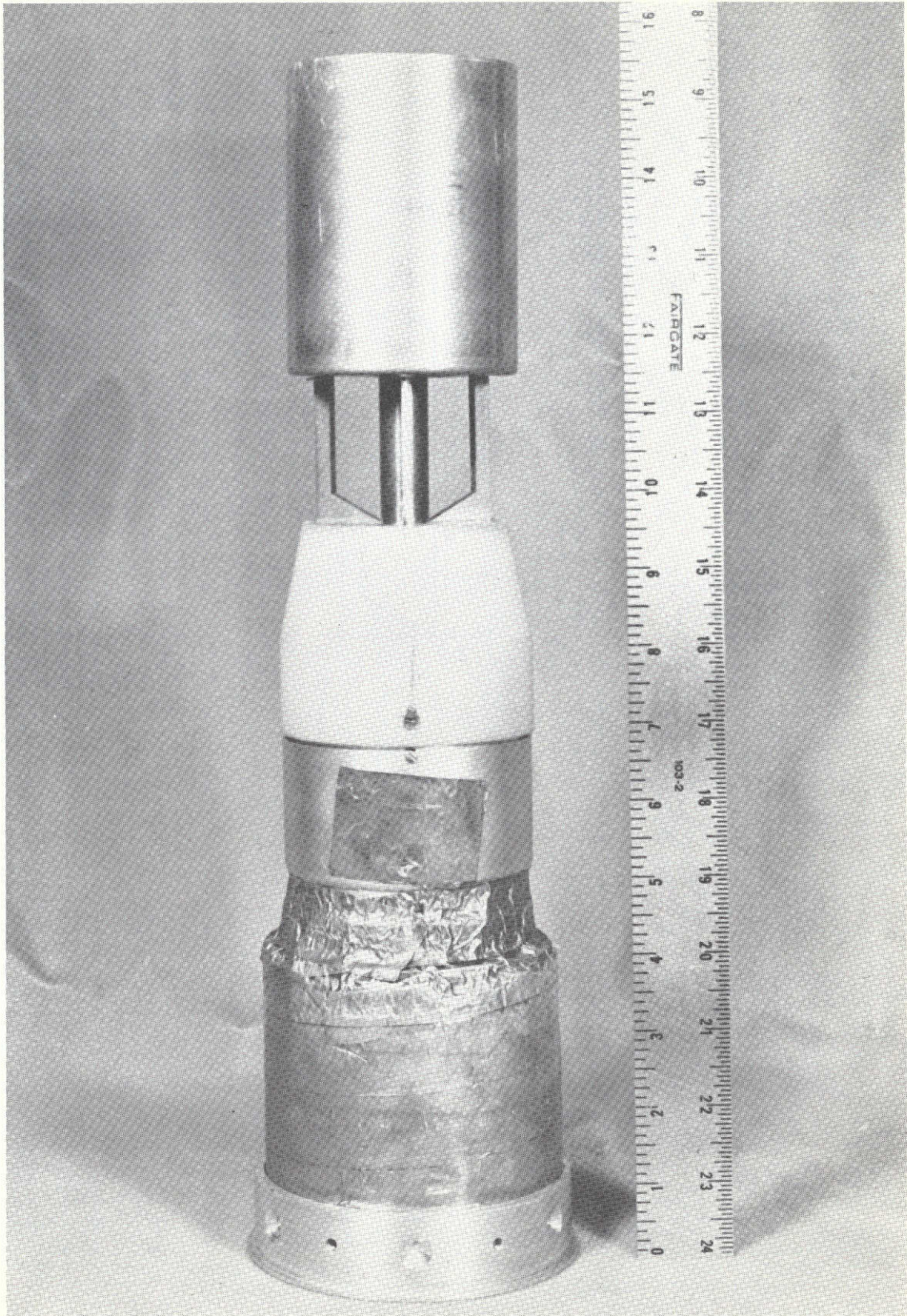


Figure 4. Gerdien Condenser/Blunt Probe Assembly.

ORIGINAL PAGE IS
OF POOR QUALITY

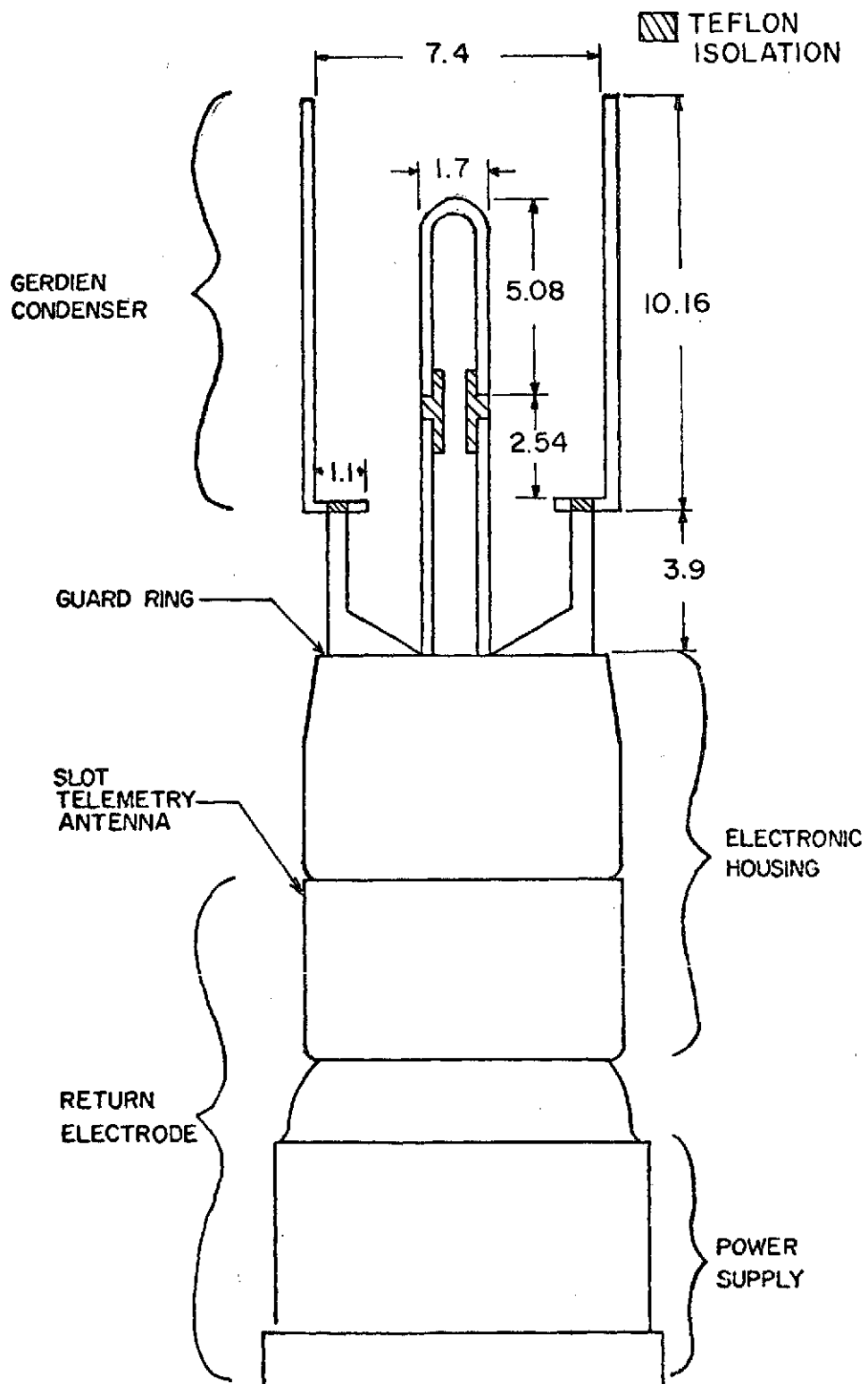


Figure 5. Schematic of the Gerdien Condenser Assembly. Dimensions are given in Centimeter.

the same potential as the collector in this configuration.

In order to keep the wiring at a minimum and avoid r-f interference, the electronics for the electrometer are seated directly behind the guard ring and are shielded in a small aluminum cup. The remaining electronic subsystems and telemetry transmitter are contained inside the antenna can. Erie RFI filters are used for electrical connection through the can to the electrometer. A nylon spacer electrically separates the collector from the larger return electrode, which is comprised of the aluminum antenna can and power supply wrapped with copper tape (Figure 4). The antenna can is mounted to the power supply by cylindrical spacers. The other side is attached to the base plate which connects the payload to the parachute and provides the mating of the payload with the nose cone and rocket motor.

This Gerdien condenser/blunt probe assembly, which has a height from base plate to the top of outer cylinder (see Figure 4) of 39.37 cm and weighs 4.5 pounds, is compatible for flying on the Arcas rocket, a vehicle used by the Meteorological Rocket Network (MRN).

3.2 Instrumentation

Figure 6 shows a block diagram of the Gerdien condenser system. A brief discussion follows of the sub-system diagrams shown in Figures 7 to 10.

3.2.1 Sweep Voltage Generator

By applying a voltage waveform across the two electrodes of the Gerdien condenser and measuring the current collected, it is possible to calculate the charge particle concentrations and mobilities in the surrounding medium. The voltage waveform used for the Gerdien condenser

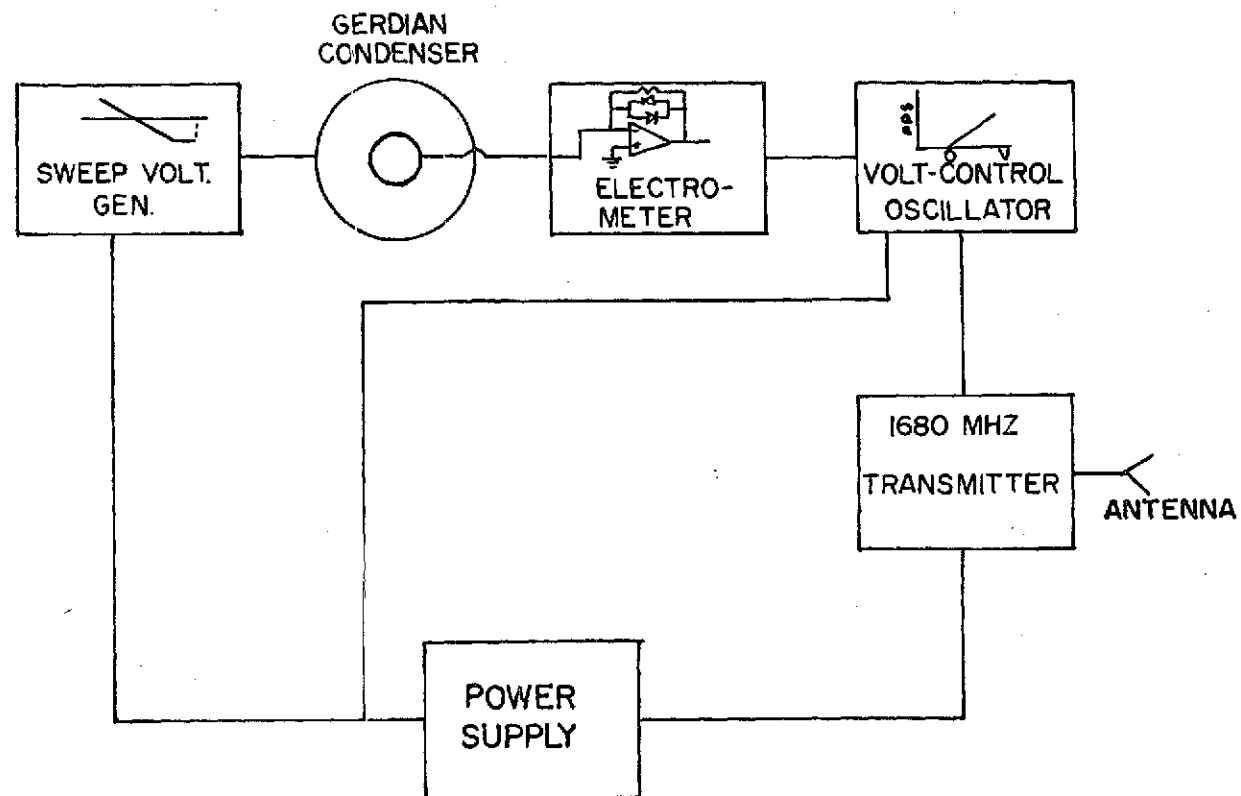


Figure 6. Schematic of the Gerdien Condenser Instrumentation.

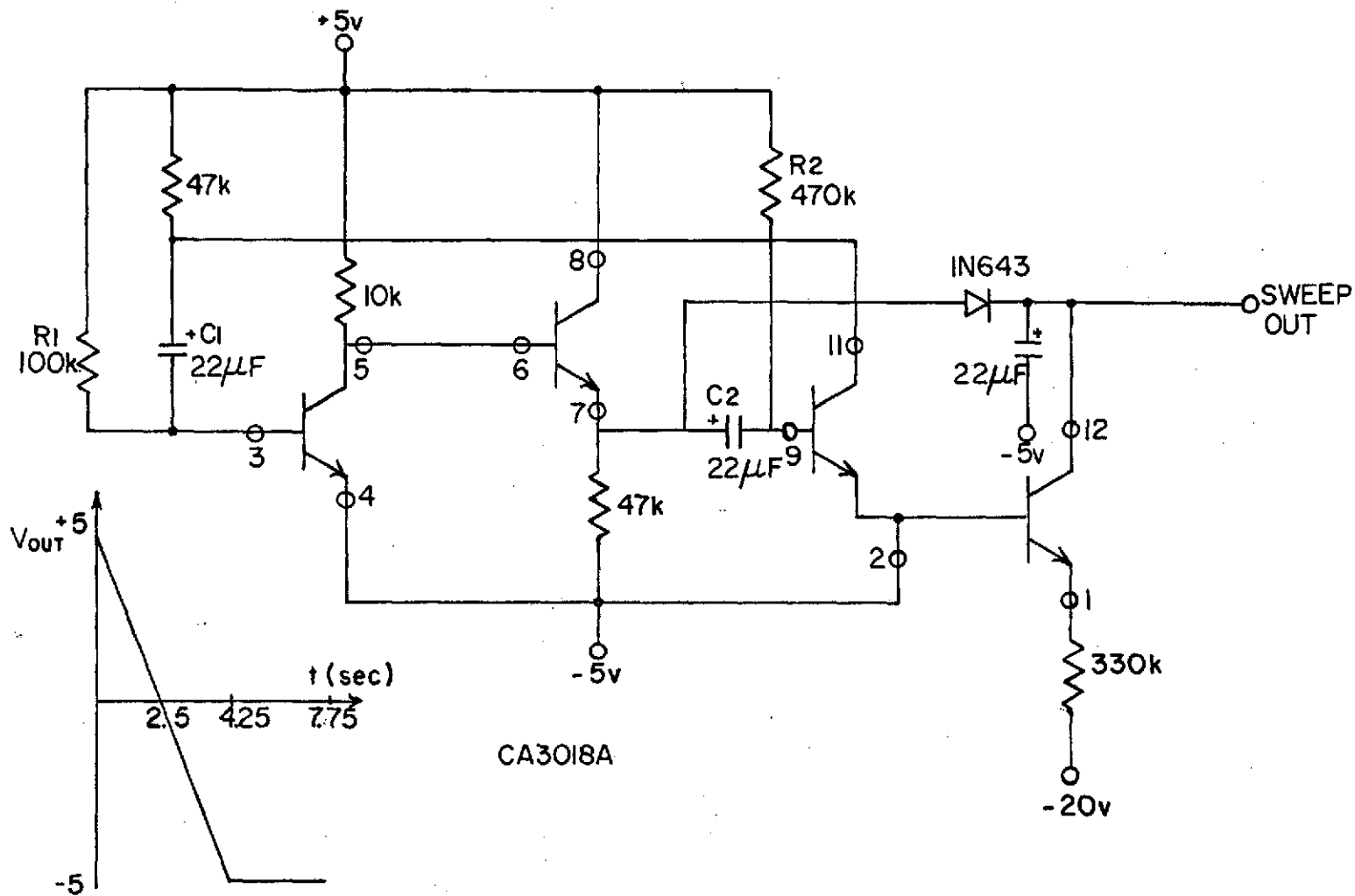


Figure 7. Sweep Voltage Generator Circuit.

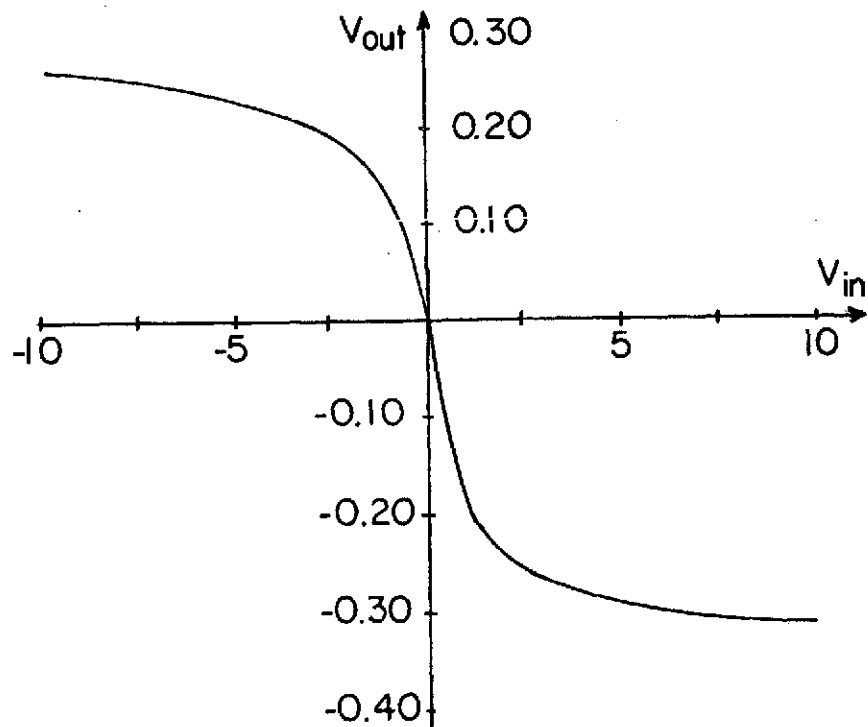
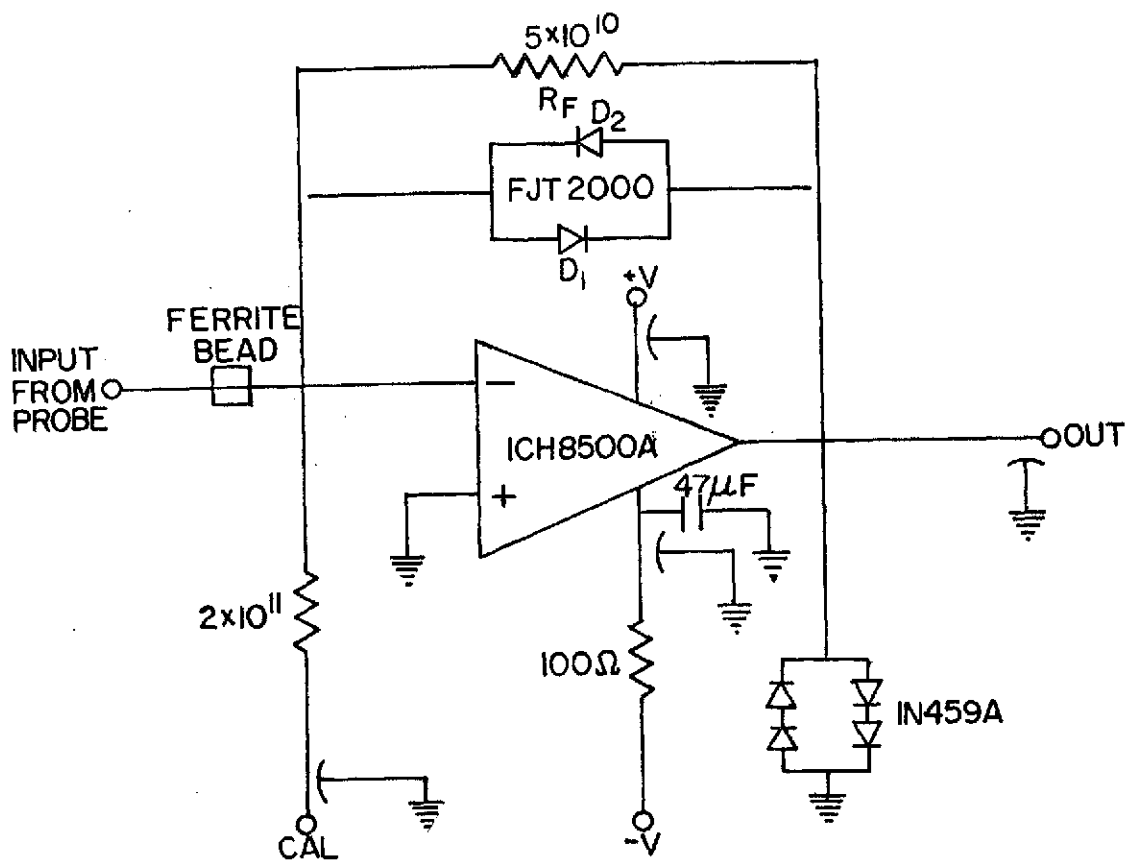


Figure 8. Logarithmic Electrometer Circuit.

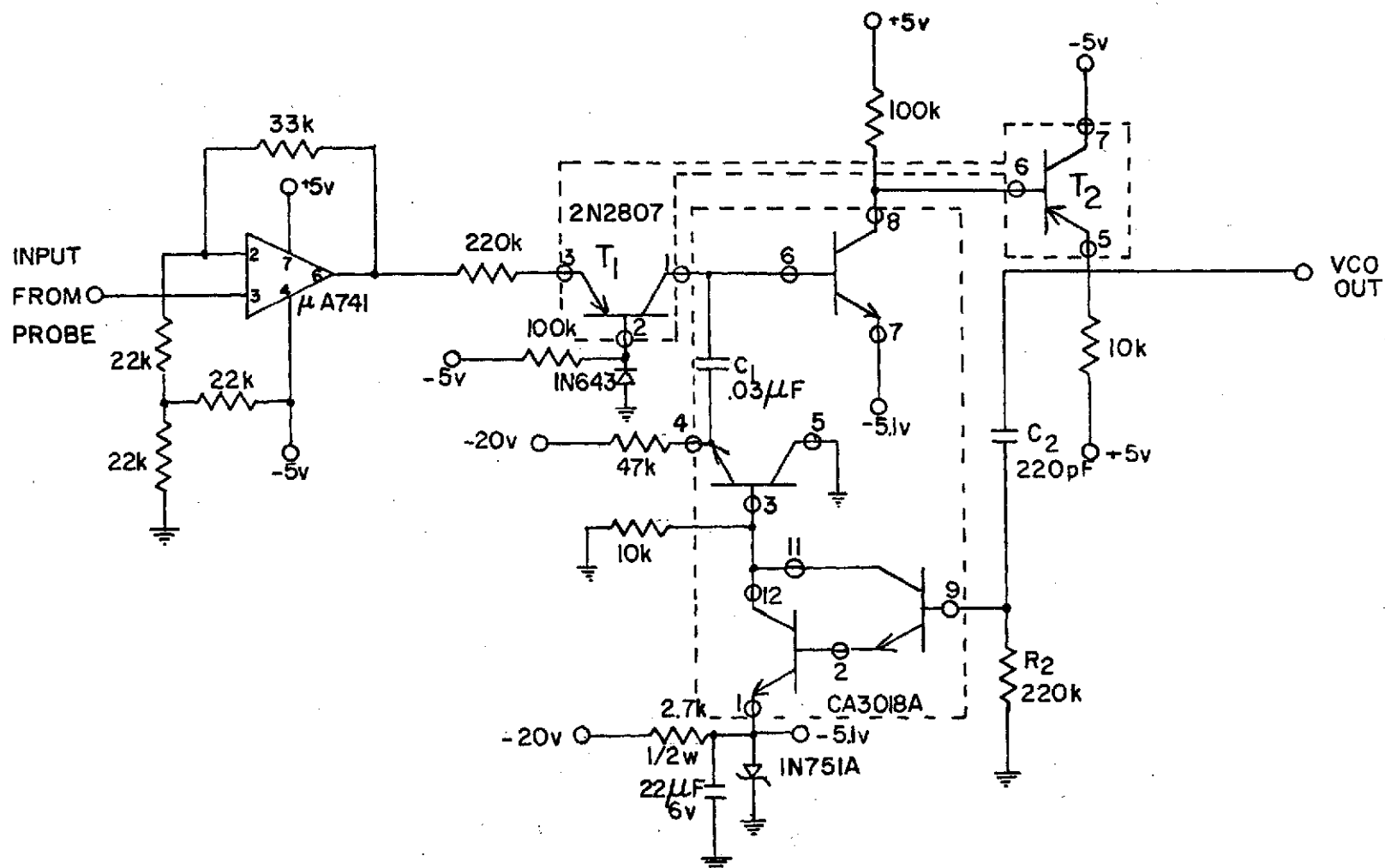


Figure 9. Voltage Controlled Oscillator Circuit.

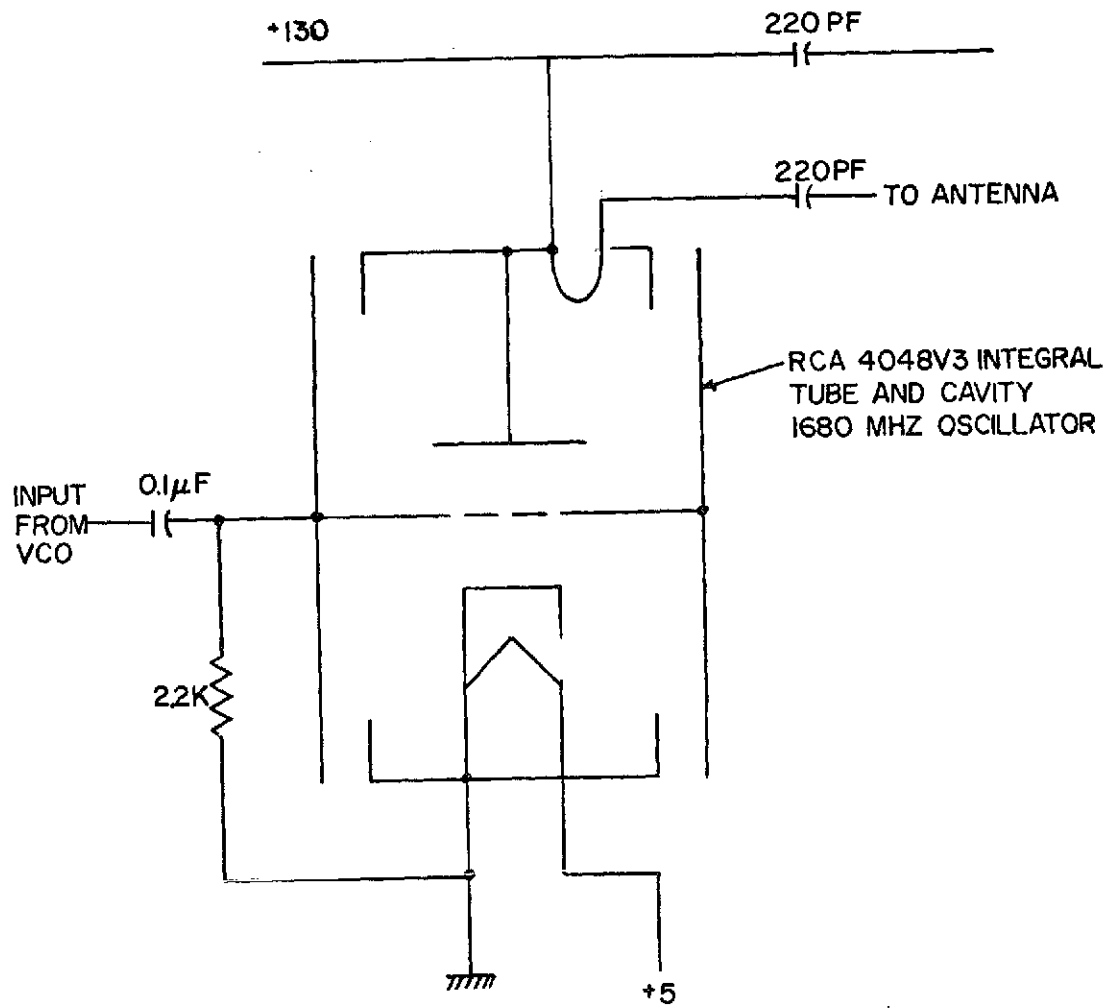


Figure 10. Transmitter Circuit.

in this particular experiment and electronics used to generate it is shown in Figure 7.

The sweep voltage generator is basically a free running (astable) multivibrator followed by a constant current run-down circuit which provides a negative-going ramp function for the output voltage when the output of the multivibrator is negative. The output of the multivibrator has a positive on-time determined by R_1C_1 with an amplitude of +5 volts followed by a negative pulse of amplitude -5 volts whose time duration is controlled by R_2C_2 . The transistors in the circuit are contained on a single integrated circuit chip (RCA3018A).

3.2.2 Electrometer

The electrometer is a highly sensitive ammeter used to measure very small currents to the collector of the instrument. A circuit diagram and its output response is given in Figure 8.

The electrometer operational amplifier is an Intersil hybrid (ICH8500A), which has extremely low input bias current. The dual diodes D_1 and D_2 (FJT2000) generate the logarithm response for positive and negative output voltages, respectively. The resistor R_F ($10^{10}\Omega$) provides a linear characteristic for small currents. The 1N459A diodes are used to protect the MOSFET input of the electrometer.

3.2.3 Voltage Controlled Oscillator (VCO)

The voltage controlled oscillator, shown in Figure 9, transforms the output voltage of the electrometer into a pulse train waveform suitable for modulating the 1680 MHz transmitter tube. A simple PPM-AM modulating system is used in telemetering the data back to ground.

The operational amplifier at the input is used as a level shifter.

The output of this circuit is pulses with constant amplitude of -5 volts whose on-time is determined by R_2C_2 . The off-time depends on the charging rate of C_1 which is linearly proportional to the collector current of transistor T_1 . The use of emitter follower (transistor T_2) at the output is to reduce the off time and have low output impedance.

3.2.4 Telemetry System

The telemetry system makes use of the RCA 1680 MHZ integral tube and cavity transmitter which directly feeds a 0.925λ circular slot antenna. The voltage controlled oscillator pulses off the transmitter at a rate of 0-200PPS. This form of modulation is compatible with the GMD/TMQ-5 receiving system, designed for radiosonde balloon data acquisition and is commonly used by the Meteorological Rocket Network (MRN). A circuit diagram of the transmitter is given in Figure 10. A detailed discussion of the antenna characteristics is given in Ionosphere Research Laboratory Scientific Report No. 249 (Cuffin, 1965).

3.2.5 Power Supply

Four 1.25 volts series-connected nickel cadmium batteries provide voltage for operating the previously mentioned Gerdien condenser electronics-excluding the transmitter tube and cavity. A (DC to DC) converter is used to provide +130 volts and -20 volts for the electronics.

CHAPTER IV

AERODYNAMICS CONSIDERATIONS

4.1 Flow Regimes

The classical theory of the Gerdien condenser discussed in Chapter 2 is based on the assumption that the instrument operates in a continuous medium. The continuous regime obtains when the mean free path is much smaller than the characteristic length which for the Gerdien condenser is the diameter of the outer cylinder. Stated more precisely, the collision-controlled regime occurs when the Knudsen number $K_n \leq .01$, where K_n is the ratio of mean free path to the diameter Conley (1974). The mean free path calculated (Maris, 1929) is plotted against the altitude in Figure 11. Figure 12 shows the flow regime for the Gerdien condenser under the investigation. Below 67 km, as is shown in the Figure, the mean free path is small compared to the diameter of the condenser, and therefore gas dynamics is sufficient for the aerodynamic calculation. Since the experimental data obtained in this work lies in this height region, the aerodynamic property of the condenser operating in this altitude range will be discussed in detail in the next sections. However, it is appropriate here to describe briefly the fluid dynamic characteristics of the other regimes shown in Figure 12.

In the region between about 67 km and 102 km the mean free path is small but not negligible compared to the characteristic length of the condenser. The gas molecules velocity, in contrast to the continuous regime, is no longer zero on the solid surface of the instrument. The gas molecules either move on it with a definite velocity or are reflected

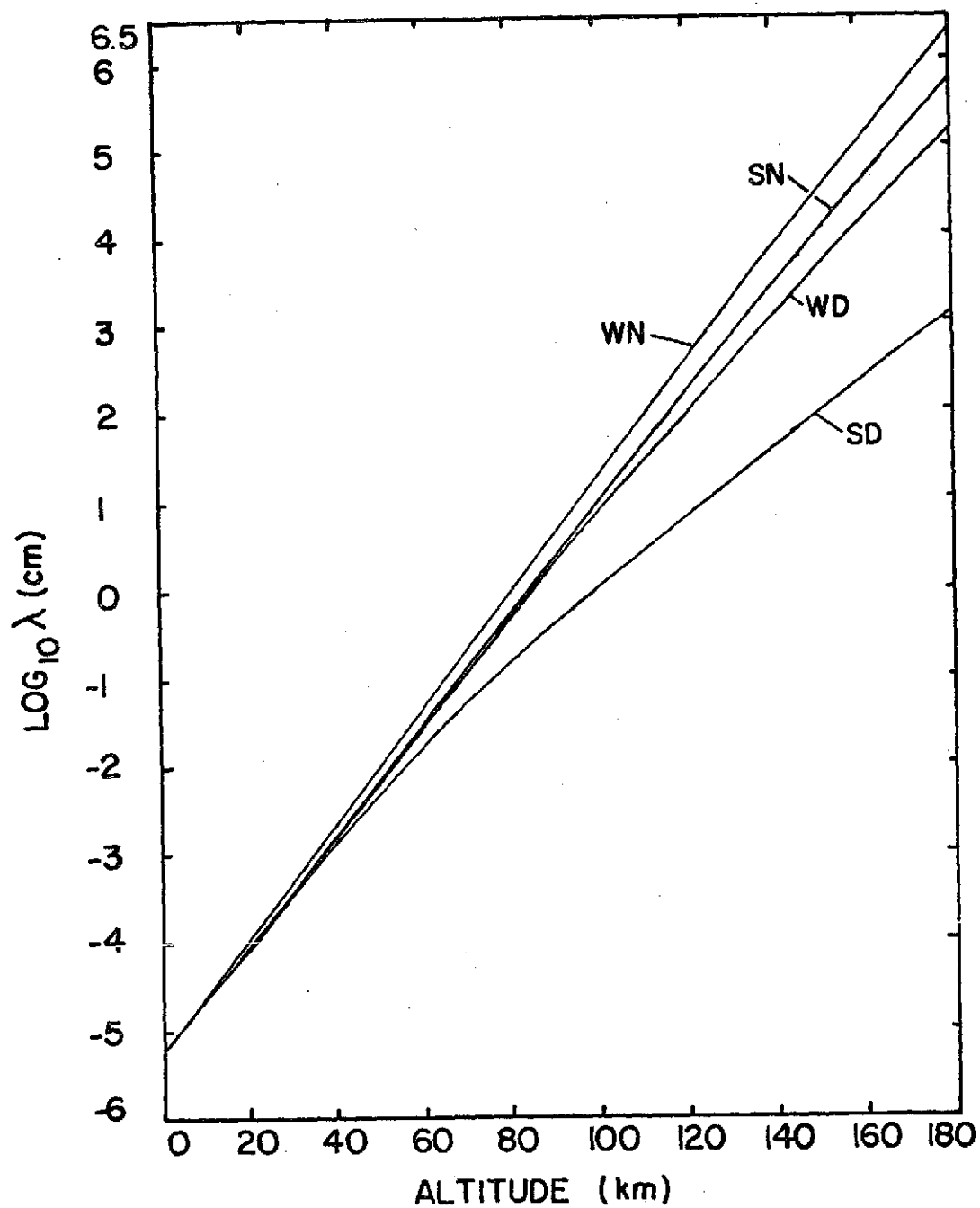


Figure 11. Variation of Mean Free Path with Altitude
(after Maris, 1929).

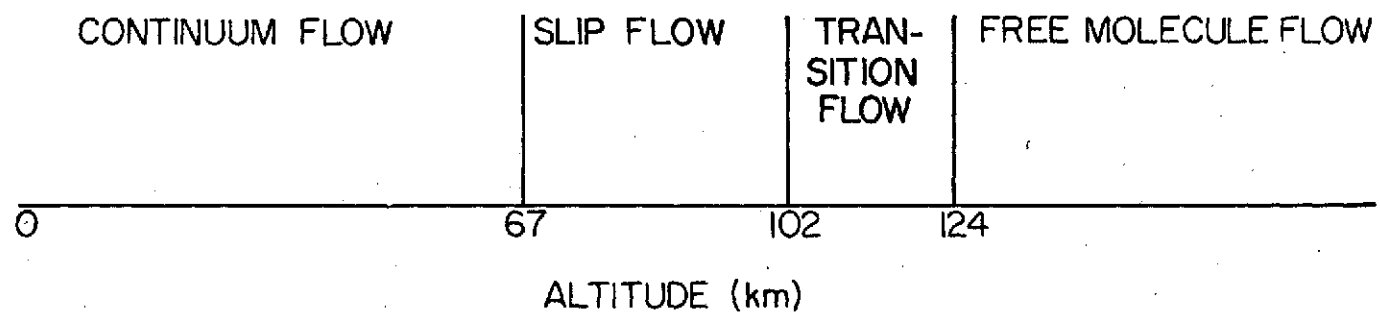


Figure 12. The Flow Regimes for the Gerdien Condenser.

from the surface or both, depending upon the smoothness of the solid surface (Kennard, 1938). An ordinary treatment of the problem is no longer satisfactory, the problem must be solved based on the kinetic theory of the gases.

In the free molecular regime (above 124 km) the mean free path is much greater than the characteristic length of the condenser. An analysis based on a Maxwellian velocity distribution for this situation seems satisfactory (Tsien, 1946).

The mean free path in the transition flow is of the same order of magnitude as the diameter of the outer cylinder, therefore, the collisions between molecules are of comparable importance to the collisions of molecules with the surface. The problem is extremely complicated and a satisfactory theoretical solution has not yet been obtained.

Therefore, when the probe is operating in a region where the continuous flow concept is not applicable, a theoretical calculation of velocity distribution in the condenser is very complicated. Although by using a condenser with larger diameter, it is possible to extend the altitude region where the continuous flow concept is applicable, there are practical limitations to this.

4.2 Compressibility Effect

As pointed out in the last section the gas dynamic treatment of the flow in the collision-controlled regime is sufficient to explain the flow properties of the condenser. For air with subsonic velocity and small density variation with pressure and temperature, the compressibility effect is usually neglected. To a first approximation the

compressibility error can be estimated with the relation:

$$\frac{n_o}{n} = \frac{\rho_o}{\rho} = \left[1 + \left(\frac{\gamma-1}{2} \right) M^2 \right]^{\frac{1}{\gamma-1}}$$

which results from a consideration of the density change in the medium caused by adiabatically bringing it to rest (Liepmann and Roshko, 1957). In this equation n is the number density; ρ is the mass density; the subscript zero denotes the condition far from the probe; $\gamma = 1.4$ is a constant; and M is the Mach number which is the ratio of the velocity of the probe-parachute assembly to the velocity of the sound. The compressibility error is very small at lower altitudes (about 0.09 percent at 30KM) and increases with altitude (about 12.5 percent at 67 km).

Whether the air flow through the condenser is laminar or turbulent depends on the Reynolds number. It can be derived from the general definition of Reynolds number, $\frac{4h\bar{U}}{\nu}$, where h is hydraulic mean depth (defined as the area of the cross-section divided by the perimeter); \bar{U} is the average velocity over a cross-section; and $\nu = \frac{\mu}{\rho}$ is the kinematic viscosity. Thus the Reynolds number for the Gerdien condenser is:

$$R_E = \frac{2(R_o - R_i)\bar{U}}{\nu} \quad (4.1)$$

Using the probe descent velocity (U) from Figure 13 and the values of coefficient of viscosity (μ) and mass density (ρ) from U. S. Standard Atmosphere Supplements (1966), the Reynolds number R_E has been plotted against altitude in Figure 14. If the Reynolds number is less than a critical Reynolds number, the flow is laminar. The critical Reynolds number must be determined experimentally; its value for two

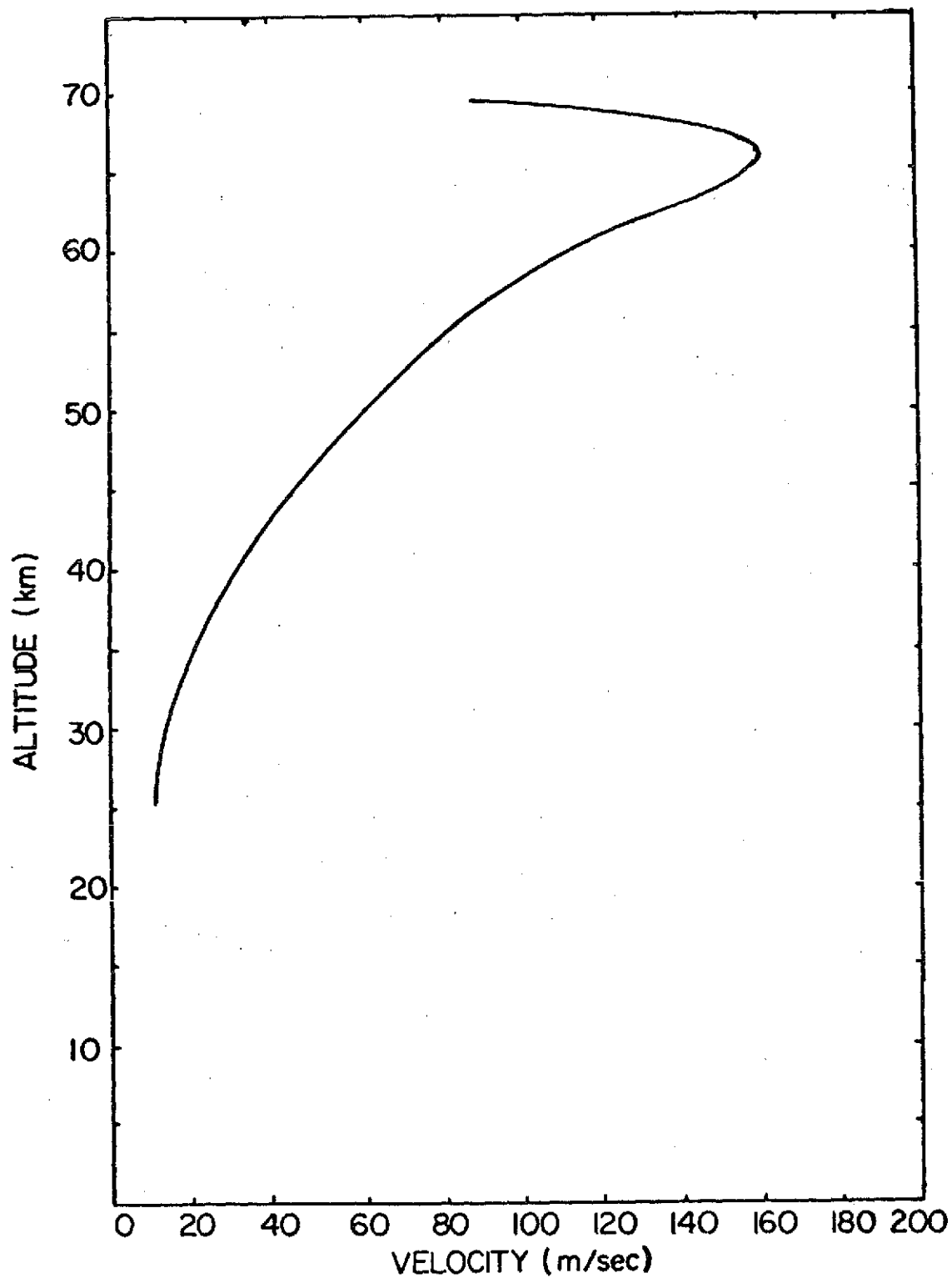


Figure 13. Descent Velocity as a Function of the Altitude
(11 January, 1974).

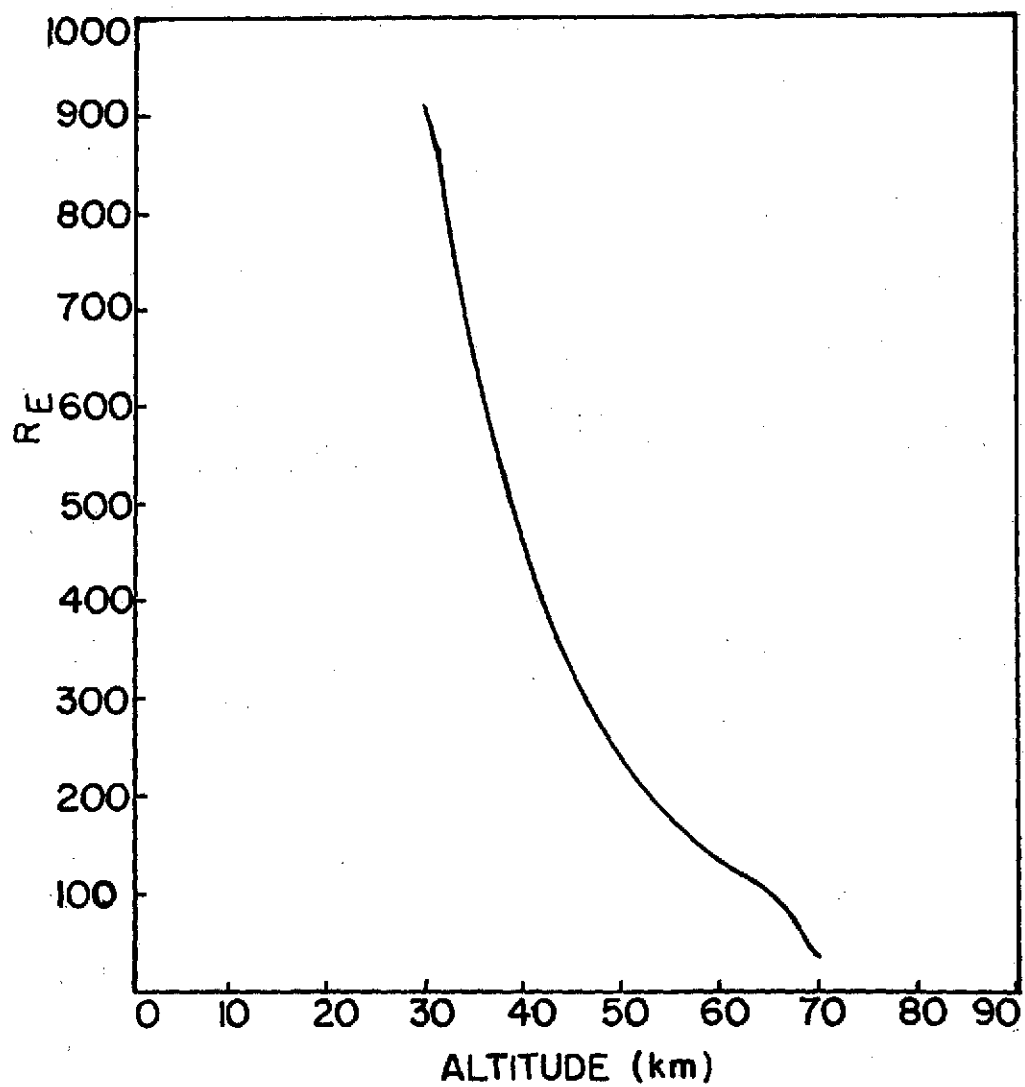


Figure 14. Variation of the Gerdien Condenser Reynolds Number with Altitude.

very long concentric cylinders is 2000 (Bird, Stewart and Lightfoot, 1960). If this number be adopted as the critical Reynolds number for the Gerdien condenser, then the air flow through the condenser is laminar (see Figure 14).

4.3 Velocity Distribution

The flow condition in a short Gerdien condenser ($L = 10.16$ cm) corresponds roughly to that in the "inlet length" of a long pipe and is a highly complicated function of Reynolds number and tube length (Paltridge, 1965). Figure 15.a shows schematically the flow condition in the inlet of a long pipe. At the entrance a very thin boundary layer is formed around the wall of the pipe. The thickness of this layer increases downstream in the pipe until it becomes equal to the radius of the pipe. Until this happens there is a core of fluid unaffected by viscosity. Since the boundary layer thickness increases as air flows deeper into the pipe, and because of constancy of flux at any cross-section, this core is accelerated. When the viscosity effect occupies the whole cross-section of the pipe, a fully established laminar flow will be developed which has a parabolic velocity distribution (Shames, 1962). By analogy, the flow condition at the inlet of two long concentric cylinders has been shown in Figure 15.b. Note that in case of the concentric cylinders two different boundary layers are present; however, as long as there exists a core uninfluenced by viscosity, the velocity distribution in the core and boundary of outer cylinder must be the same as of a pipe with similar size and geometry.

To determine the inlet length (core length) of flow in the condenser the so called "Schiller's Method" will be followed. A detailed discussion of this method can be found in Goldstein (1938). Assuming

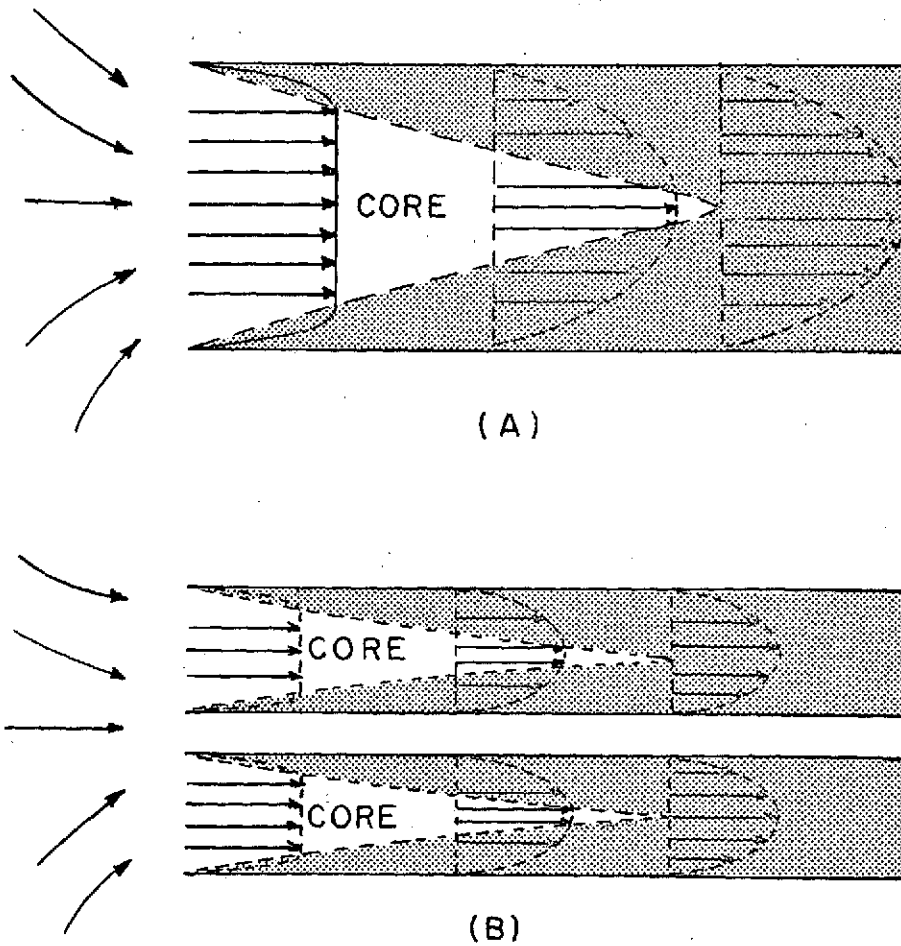


Figure 15. Flow Conditions: (A) in Inlet of a Pipe, (B) in Inlet of Concentric Cylinders (after Shames, 1962).

that boundary layer has a thickness δ at any cross-section the relation:

$$\frac{U}{U_1} = 2 \frac{y}{\delta} - \frac{y^2}{\delta^2}$$

can be written. Where U_1 is the velocity in the core and $y = R_o - r$. This relation along with equation of continuity and momentum equation give the following relation between x and U_c :

$$\frac{x}{R_o R_E} = f(\chi)$$

and:

$$\chi = \frac{U_c}{\bar{U}_p} - 1 \quad (4.2)$$

where x is the distance measured from the entrance; U_c is the core velocity; and \bar{U}_p is the average velocity in the fully stabilized laminar flow region. Figure 16 shows the variation of $f(\chi)$ with χ which has been reproduced from Goldstein (1938). In case of flow in a pipe it is well known that the maximum velocity U_{max} is twice the average velocity \bar{U}_p in the parabolic region; then by letting $U_c = U_{max} = 2\bar{U}_p$, $\chi = 1$ and the value of $f(\chi)$ can read from the figure ($f(\chi) = .0575$), and hence:

$$x = .0575 R_o R_E$$

In case of concentric cylinders the equality $U_{max} = 2\bar{U}_p$ is no longer true, however, a relation between U_{max} and \bar{U}_p can be found assuming a steady incompressible laminar flow through the condenser. The Navier-Stokes equation in cylindrical coordinates can be written as:

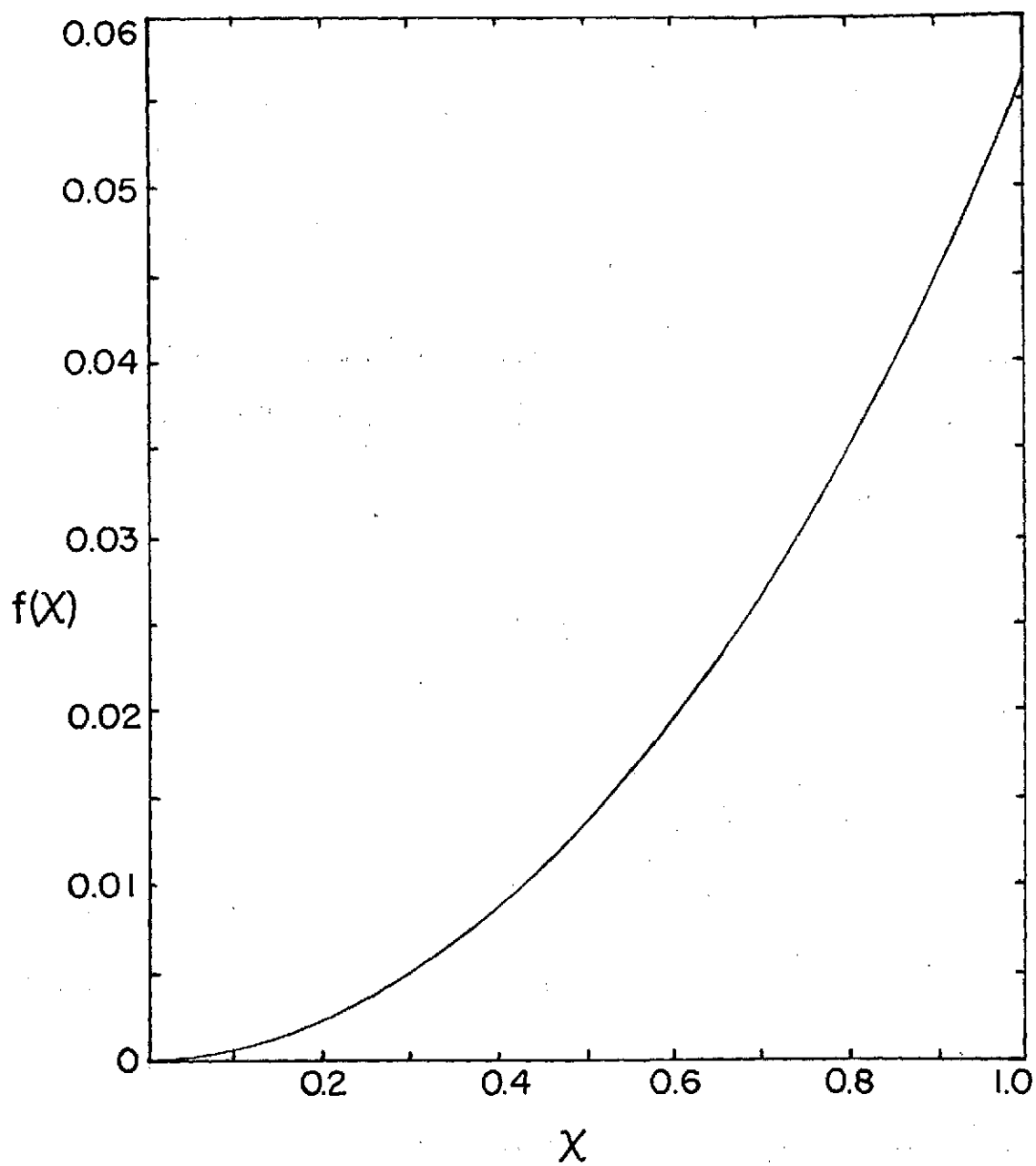


Figure 16. Variation of $f(\chi)$ with χ (after Goldstein, 1938).

$$\frac{\partial^2 U_x}{\partial r^2} + \frac{1}{r} \frac{\partial U_x}{\partial r} = - \frac{1}{\mu} \frac{dP}{dx} \quad (4.3)$$

which integrates to:

$$\frac{\partial U_x}{\partial r} = - \frac{dP}{dx} \frac{r}{2\mu} + \frac{c_1}{r} \quad (4.4)$$

integrating again:

$$U_x = - \frac{dP}{dx} \frac{r^2}{4\mu} + c_1 \ln r + c_2 \quad (4.5)$$

where c_1 and c_2 are constants of integration and can be evaluated by applying boundary conditions $U_x = 0$, at $r = R_o$ and at $r = R_i$:

$$c_1 \ln R_o + c_2 = \frac{dP}{dx} \frac{R_o^2}{4\mu}$$

$$c_1 \ln R_i + c_2 = \frac{dP}{dx} \frac{R_i^2}{4\mu}$$

or:

$$c_1 = \frac{\frac{R_o^2}{4\mu} - \frac{R_i^2}{4\mu}}{\ln \frac{R_o}{R_i}} \frac{dP}{dx} \quad (4.6)$$

$$c_2 = \frac{\frac{R_i^2}{4\mu} \ln R_o - \frac{R_o^2}{4\mu} \ln R_i}{\ln \frac{R_o}{R_i}} \frac{dP}{dx} \quad (4.7)$$

The average velocity in the parabolic region is:

$$\bar{U}_p = \bar{U}_x = \frac{\int_0^{2\pi} \int_{R_i}^{R_o} U_x r dr d\theta}{\int_0^{2\pi} \int_{R_i}^{R_o} r dr d\theta} \quad (4.8)$$

which after substituting the value of U_x from equation (4.5) with c_1 and c_2 as given in equations (4.6) and (4.7) integrates to:

$$\bar{U}_p = \bar{U}_x = \left[-\frac{R_o^2 + R_i^2}{8\mu} + \frac{R_o^2 - R_i^2}{4\mu \ln \frac{R_o}{R_i}} \left(\frac{R_o^2 \ln R_o - R_i^2 \ln R_i}{R_o^2 - R_i^2} - \frac{1}{2} \right) + \frac{R_i^2 \ln R_o - R_o^2 \ln R_i}{4\mu \ln \frac{R_o}{R_i}} \right] \frac{dP}{dx} \quad (4.8)$$

The maximum velocity U_{\max} can be found by solving $\frac{\partial U_x}{\partial r} = 0$ for r , and substituting this value of r in equation (4.5):

$$\frac{\partial U_x}{\partial r} = \left(\frac{R_o^2 - R_i^2}{4\mu \ln \frac{R_o}{R_i}} \frac{1}{R_{\max}} - \frac{R_{\max}}{2\mu} \right) \frac{dP}{dx} = 0$$

or:

$$R_{\max} = \left(\frac{R_o^2 - R_i^2}{2 \ln \frac{R_o}{R_i}} \right)^{\frac{1}{2}}$$

and:

$$U_{\max} = \frac{-R_{\max}^2 \ln \frac{R_o}{R_i} + \left(R_o^2 - R_i^2 \right) \ln R_{\max} + R_i^2 \ln R_o - R_o^2 \ln R_i}{\frac{R_o^2 + R_i^2}{2} \ln \frac{R_o}{R_i} - \frac{R_o^2 - R_i^2}{2}}$$

therefore:

$$\chi = \frac{U_{\max}}{\bar{U}_p} - 1 = \frac{\frac{R_o^2 - R_i^2}{2} \ln \frac{R_o^2 - R_i^2}{R_o} + R_i^2 \ln \frac{R_o^2 - R_o^2}{R_o} \ln \frac{R_o}{R_i} - \frac{R_o^2 + R_i^2}{2} \ln \frac{R_o}{R_i}}{\frac{R_o^2 + R_i^2}{2} \ln \frac{R_o}{R_i} - \frac{R_o^2 - R_i^2}{2}} \quad (4.9)$$

If the value $R_o = 3.7$ cm and $R_i = 0.7$ cm be inserted in equation (4.8), then $\chi = 0.54$ and $f(\chi)$ can be read from Figure 16 ($f(\chi) = 0.017$).

With this value of $f(\chi)$ the equation (4.2) reduces to:

$$x = R_o R_E f(\chi) \approx 0.0629 R_E \quad (4.10)$$

Equation (4.10) approximately determines the distance required for fully stabilized laminar flow to be developed. The variation of x with altitude has been plotted in Figure 17. Below an altitude of about 56 km the inlet length exceeds the length of the condenser, above this height range both a core of fluid and a fully stabilized flow region exist. Because of nonlinearity in the differential equation, only a numerical calculation of velocity in the inlet is possible. Goldstein (1938), using the equation of motion and the continuity equation has numerically obtained the fluid velocity at every point in the inlet of a pipe. Figure 18 has been reproduced from Goldstein; in case of the Gerdien condenser the values of velocity for $\frac{r}{R_o}$ less than about 0.2 must be disregarded.

It has been suggested (York, 1974) that above 56 km the air velocity at the entrance may not be equal to free stream velocity; using Bernoulli's equation the velocity at the entrance can be approximately determined:

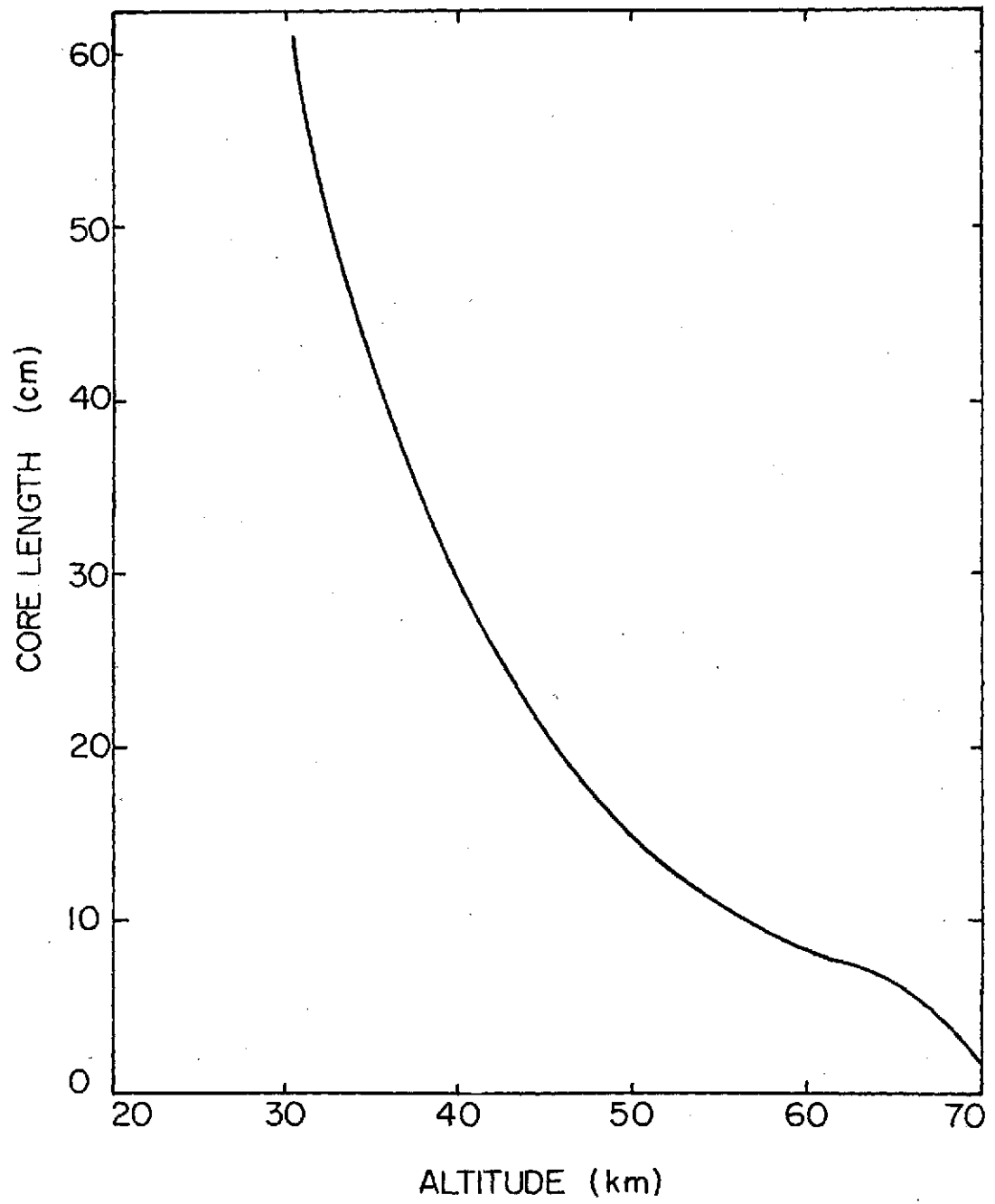


Figure 17. Variation of Flow Core-Length with Altitude.

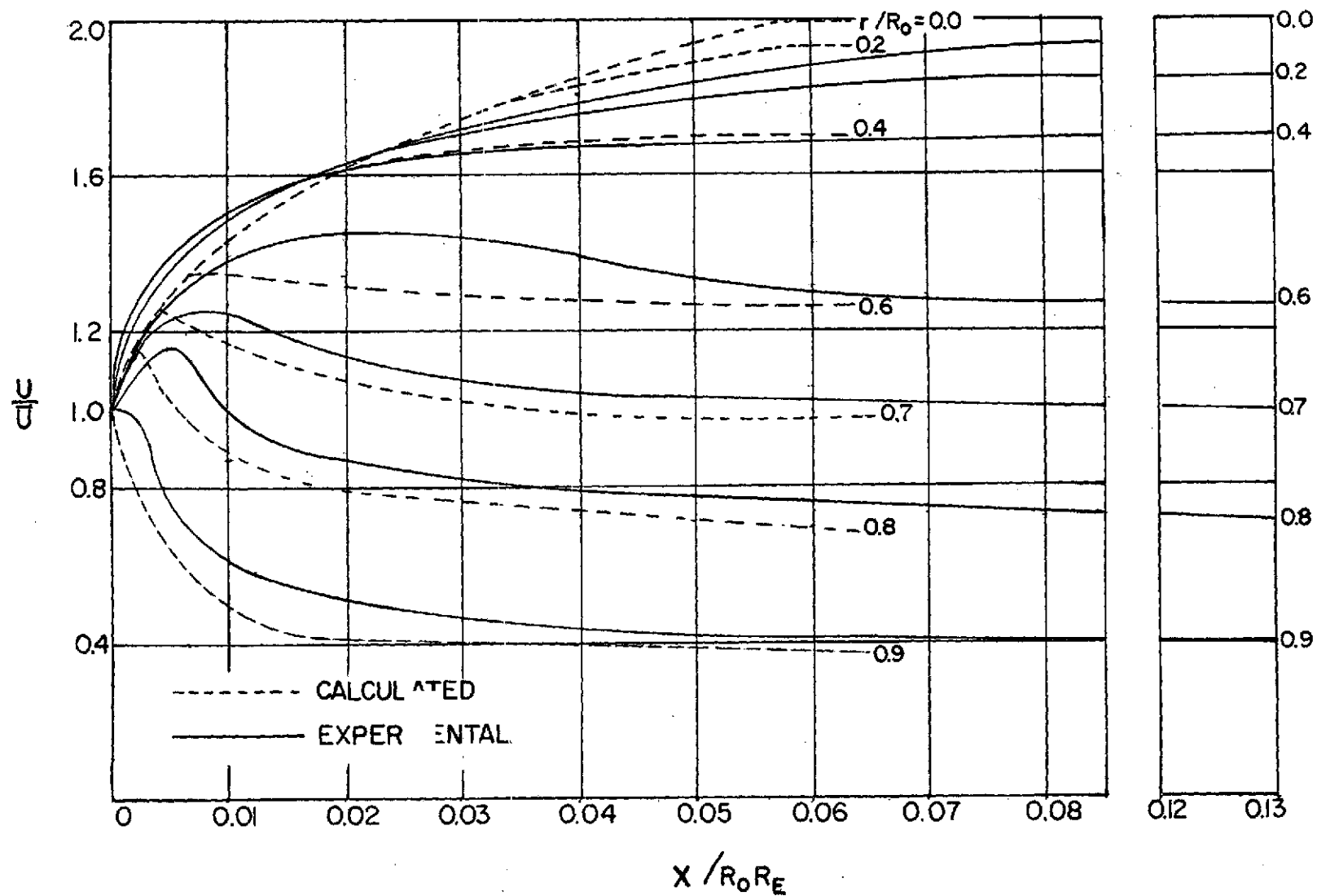


Figure 18. Entry Flow in a Circular Cylinder (after Goldstein, 1938).

$$\frac{1}{2} \rho U_{in}^2 + P_{in} = P_{atm} + \frac{1}{2} \rho U_{probe}^2 \quad (4.11)$$

where U_{in} and P_{in} are the air velocity and air pressure at the front end of the condenser, respectively; U_{probe} is the instrument velocity (free stream velocity). The pressure at the entrance may be obtained from:

$$P_{in} = P_{atm} + \Delta P_{VL} \quad (4.12)$$

where ΔP_{VL} is the pressure loss in the condenser due to the air viscosity and is given by Shames (1962):

$$\Delta P_{VL} = \frac{\bar{U}^2}{2} \frac{L}{D} \rho f \quad (4.13)$$

where f is the friction coefficient and for laminar flow is given by:

$$f = \frac{64}{R_E} \quad (4.14)$$

substituting equation (4.12) for P_{in} in equation (4.11) with ΔP_{VL} and f as are given in equations (4.13) and (4.14), respectively, the equation (4.12) can be solved for U_{in} :

$$U_{in} = \left[2\rho \left(P_{atm} - \frac{\bar{U}^2}{2} \frac{L}{D} \rho \frac{64}{R_E} \right) + U_{probe}^2 \right]^{\frac{1}{2}} \quad (4.15)$$

If it can be assumed that the average velocity is the same as the free stream velocity, U_{in} can be calculated using an atmospheric model for pressure and density (CIRA). It turns out, however, there is no significant difference between the values of U_{in} calculated from equation (4.15) and free stream velocity. From the above discussion, it can be concluded that in this case (above 56 km) the air enters the condenser

with a velocity of about the same as free stream velocity. Within the condenser two distinct flow regions exist:

- (a) An entry region with a relatively thick boundary layer in which the air flow velocity is a complex function of x and r ; and a core of fluid with air velocity as a function of x only.
- (b) A fully stabilized flow region with a parabolic velocity distribution which its average is equal to the free stream velocity.

Since an overall average velocity calculation is not possible, it is arbitrarily assumed that average velocity at any cross-section is the same as the free stream velocity.

When the boundary layer thickness is thin (below 56 km), the so called "displacement thickness" concept may be applied. For the outer cylinder the boundary layer thickness is much smaller than the radius, and a flat plate approximation may be used:

$$\delta_o = 1.721 \sqrt{\frac{vx}{U_c}} \quad (4.16)$$

For the inner cylinder the displacement thickness is given by Kelly (1954):

$$\delta_i = 1.721 \left(\frac{vx}{U_c} \right)^{\frac{1}{2}} \left[1 - 0.204 \left(\frac{4}{R_i} \right) \left(\frac{vx}{U_c} \right)^{\frac{1}{2}} + 0.146 \left(\frac{4}{R_i^2} \right)^2 \left(\frac{vx}{U_c} \right) \right] \quad (4.17)$$

Since δ_o and δ_i are a function of x , their average over the entire length of the condenser may be obtained as:

$$\bar{\delta}_o = \frac{3.442}{3} \sqrt{\frac{VL}{U_c}} \quad (4.18)$$

$$\begin{aligned} \bar{\delta}_i = 1.721 \left(\frac{VL}{U_c} \right)^{\frac{1}{2}} & \left[\frac{2}{3} - 0.102 \left(\frac{4}{R_i} \right) \left(\frac{VL}{U_c} \right)^{\frac{1}{2}} \right. \\ & \left. + \frac{0.292}{5} \left(\frac{4}{R_i} \right)^2 \left(\frac{VL}{U_c} \right) \right] \end{aligned} \quad (4.19)$$

Using the constancy of flux concept at any cross-section the core velocity can be calculated:

$$\pi[(R_o - \bar{\delta}_o)^2 - (R_i + \bar{\delta}_i)^2]U_c = \pi(R_o^2 - R_i^2)U_o \quad (4.20)$$

A simple iterative computer program given in Appendix A has been used to determine the values of U_c as a function of altitude; the results of this computer calculation is plotted in Figure 19 (dotted line). It must be noted, although; the average velocity in the condenser is increased considerably with comparison to the descent velocity, it will not alter the density and mobility of charge particles using the free stream velocity (since the product of velocity and area remains constant in this method).

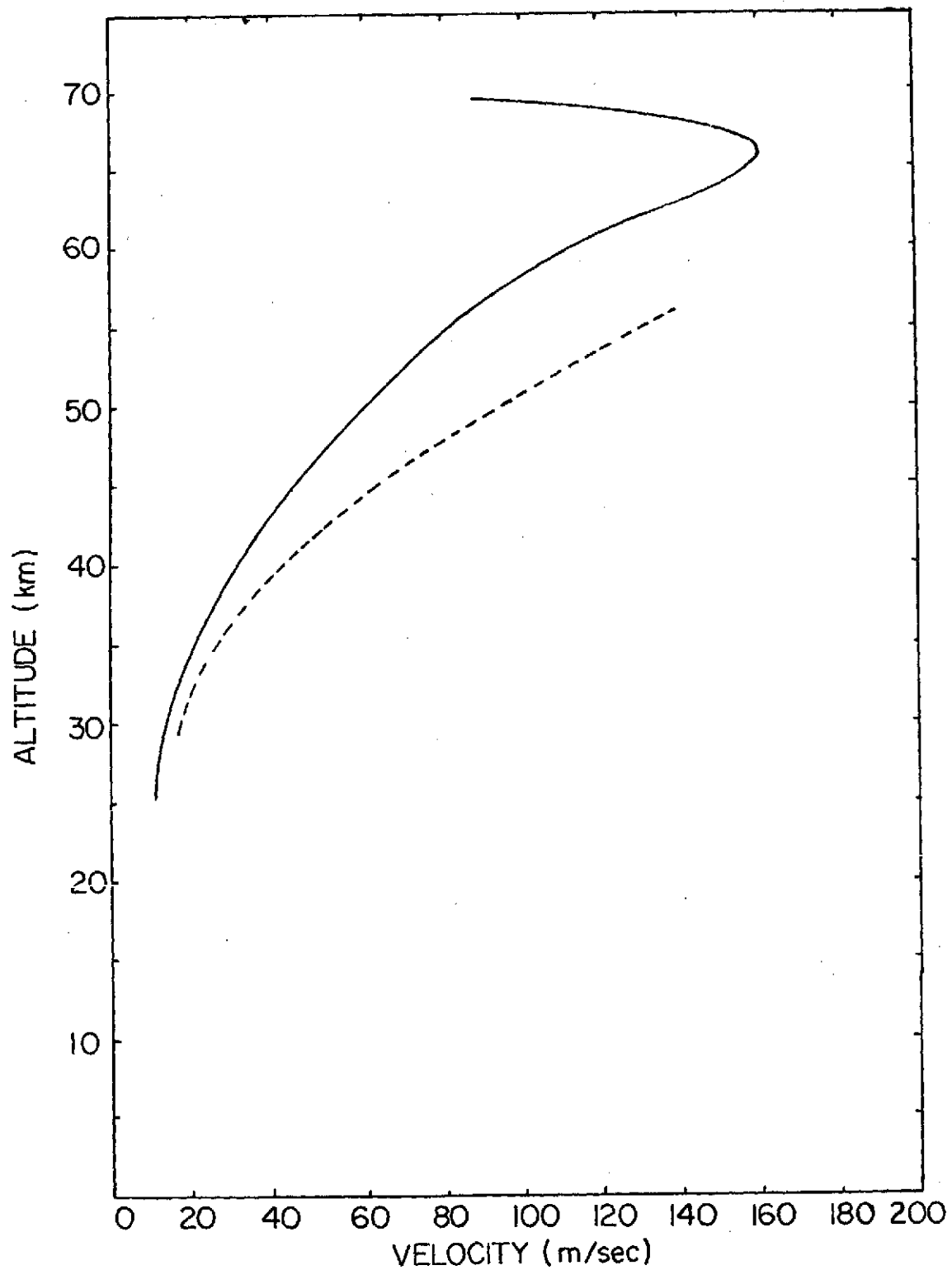


Figure 19. Descent Velocity of the Gerdien Condenser (full line) and Calculated Velocity of Air Flow (dotted line).

CHAPTER V

FLIGHTS AND DATA

5.1 The Gerdien Condenser Launch

The Gerdien condenser and associated instrumentations, which were described in chapter three, is compatible for flying on the Arcas rocket, a vehicle routinely used for wind and temperature measurement. This rocket is designed to carry a parachute-borne payload for ejection near Apogee. Three parachute-borne Gerdien condenser experiments employing the Arcas rocket as the launch vehicle were carried out. Most of the useful data obtained from these experiments occurs after expulsion from the rocket when the Gerdien condenser is descending subsonically to the earth suspended under a parachute.

The first successful Gerdien condenser flight occurred at White Sand Missile Range (WSMR), New Mexico on 11 January 1974 at 1845 UT. The flight apogee for this experiment was about 70 km. An analysis of data indicates that the angle of attack problems have been largely eliminated by the use of a more aerodynamically stable decelerating device, a starute manufactured by Space Data Corporation.

The other two flights took place at Wallops Island (WI), Virginia; one on 29 June 1974 at 2112 UT and the other on 30 June 1974 at 0315 UT. The data from these last two experiments have not yet been reduced and will not be presented in this work.

The probe is activated and calibrated on the ground just prior to launch; the preflight calibration procedure involves inserting a precision resistor between two electrodes of the probe and recording

the telemetered probe response on a magnetic tape. The calibration response of the Gerdien condenser to a sweep voltage waveform (Figure 21.a) is shown in Figure 20. While the probe is in-flight, the impedance of the surrounding medium (or conductivity) is the unknown quantity which is measured; then knowing saturation current and volume rate of air flow through the aspiration condenser both density and mobility can be determined (see Chapter II). The in-flight mode of operation (a typical strip chart record) at an altitude of about 43 km is shown in Figure 21.b.

5.2 Reduction of Data

The first step for reducing data is to draw the current-voltage characteristics from the strip chart record which represents the variation of frequency with time. This involves obtaining current from calibration response (Figure 20) and voltage from sweep voltage waveform (Figure 21.a) for different points on the strip chart. Once the current-voltage characteristic is obtained, a radar plot showing the position of the payload as a function of time (Figure 22) provide the information necessary for determining the altitude at the time of the measurement.

When sweeping the voltage to outer cylinder in the Gerdien condenser, a displacement current will go to the electrometer. This current is given by the equation

$$i_d = c \frac{dv}{dt} \quad (5.1)$$

where c is capacity between central electrode and electrometer and $\frac{dv}{dt}$ is constant for a ramp voltage sweep. The displacement current was

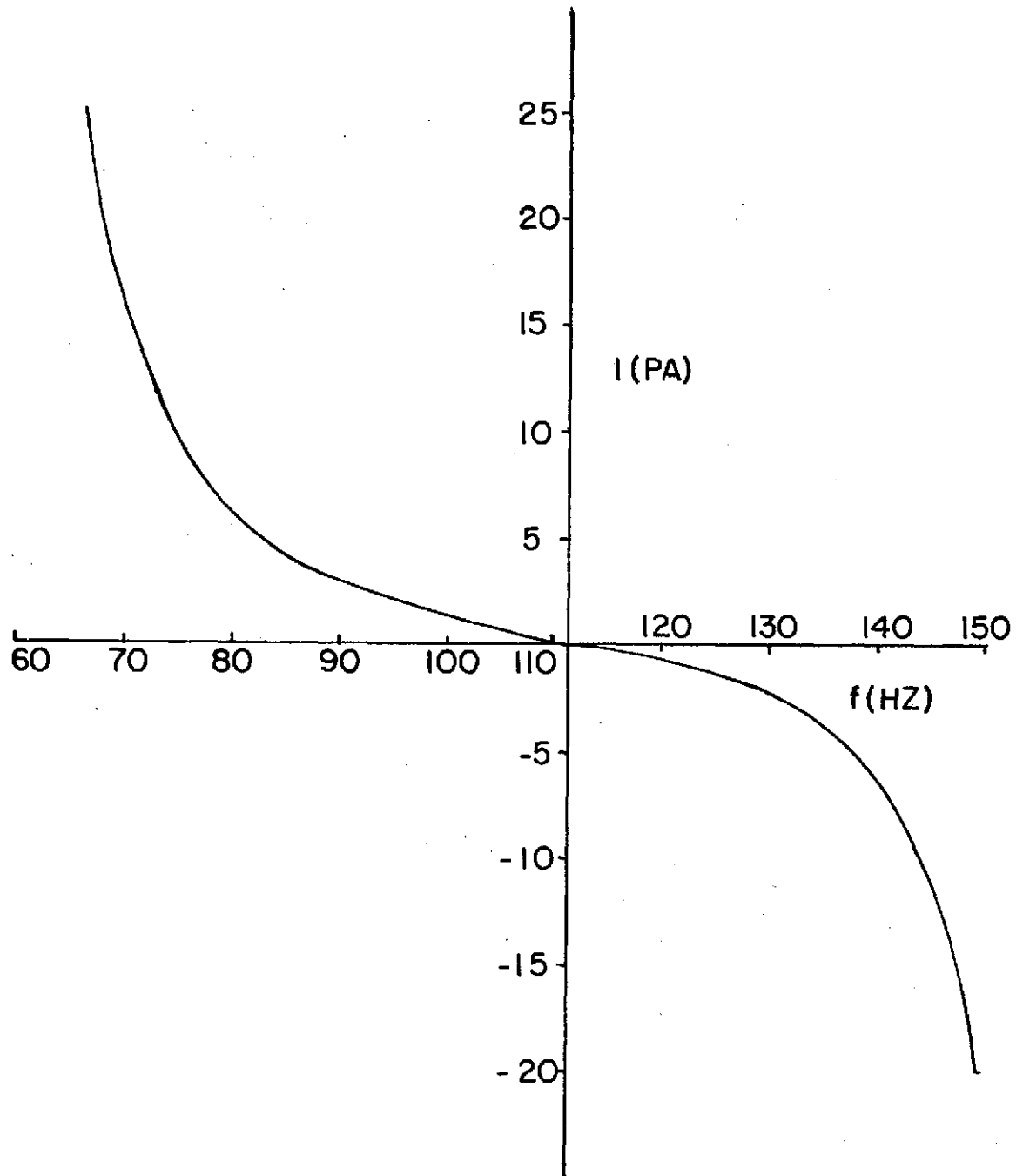


Figure 20. Calibration Current as a Function of Frequency.

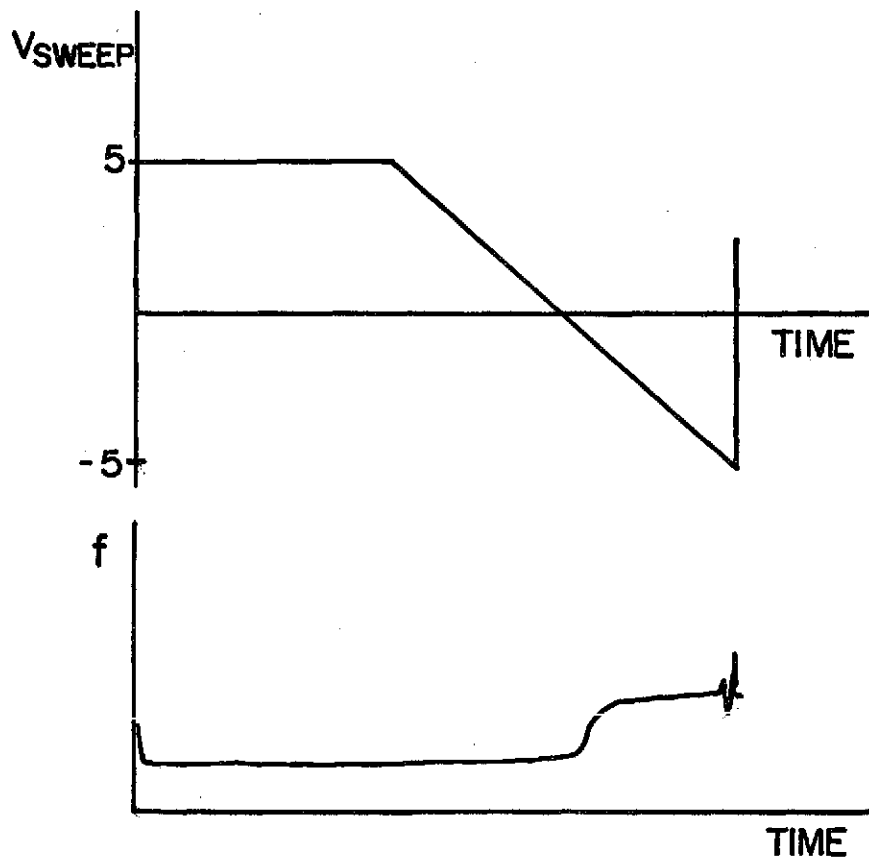


Figure 21. The Gerdien Condenser Sweep Waveforms:
(a) Applied Sweep Voltage, (b) Strip
Chart Record.

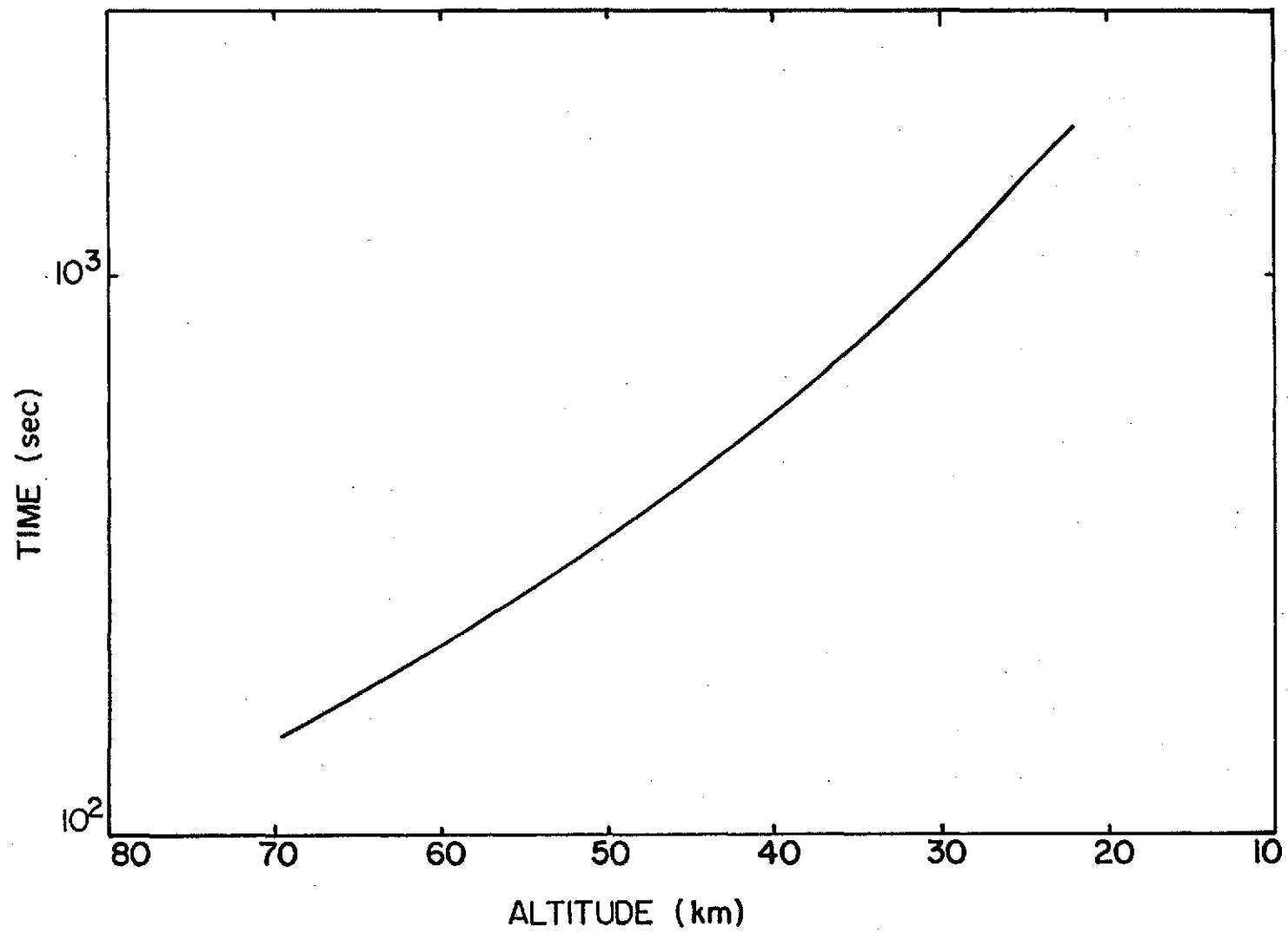


Figure 22. Descent Time as a Function of Altitude.

calibrated before flight and has a value of 1.2 PA.

Figure 23 shows two different current-voltage characteristics of the Gerdien condenser obtained from the strip chart record for altitudes of about 62 km (Figure 23.a) and 39 km (Figure 23.b). The effect of displacement current has been taken into account in drawing the current-voltage characteristic; it has been added to a positive collector current and has been subtracted from a negative one. Two distinct slopes of the current-voltage characteristic in Figure 23.a indicate the presence of two groups of ions with different mobilities; the current-voltage characteristic of the Gerdien condenser above about 47 km is of this type. The Gerdien condenser characteristic in altitude range between 38 km and 47 km is similar to the one shown in Figure 23.b; hence, a spectrum of positive ions with different mobilities must be present in this altitude range.

For calculating the positive ion densities and their relevant mobilities, the equations:

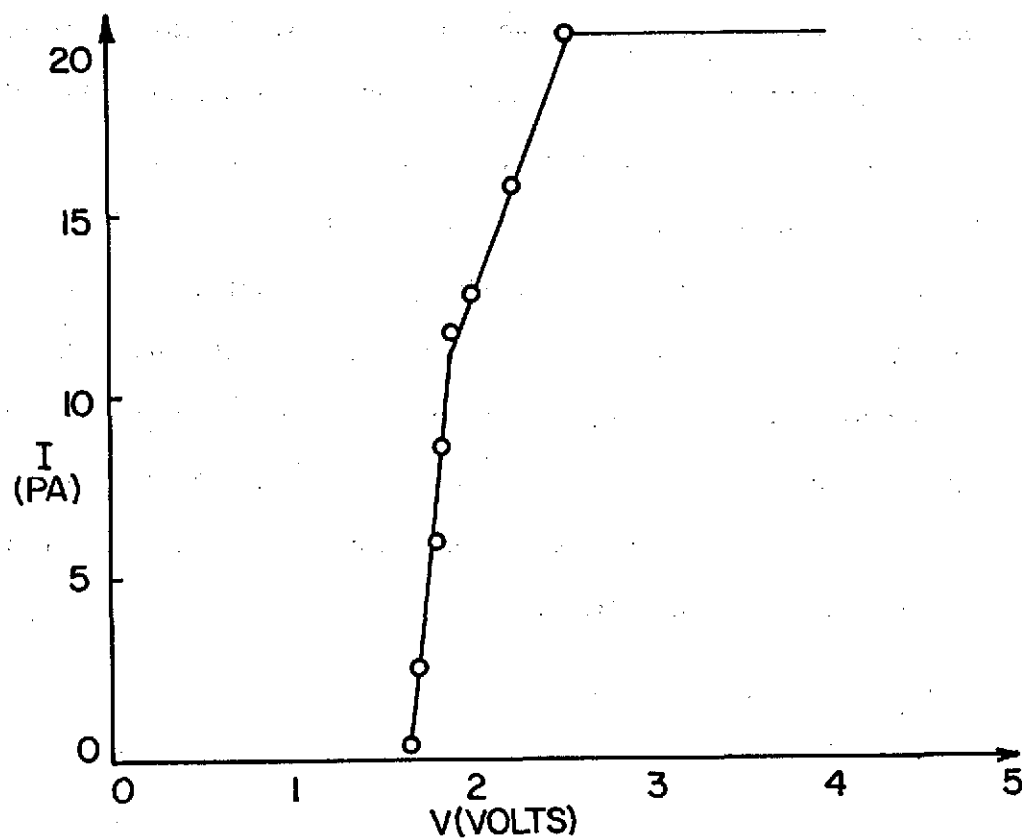
$$N^+ = \frac{i_o^+}{e\pi(R_o^2 - R_1^2)\bar{U}} \text{ for } V > V_o \quad (5.2)$$

and:

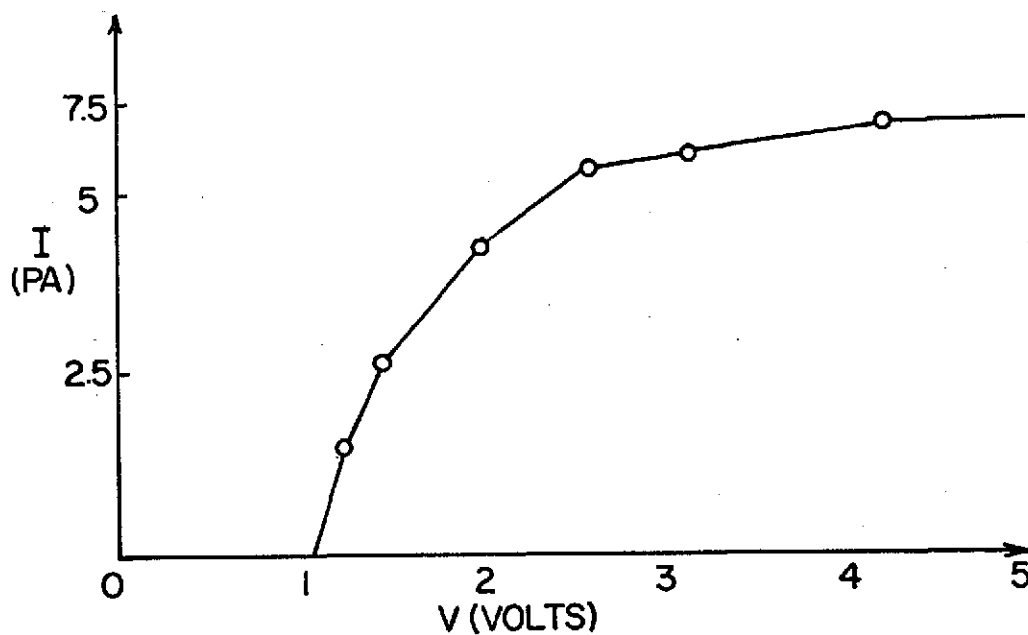
$$k^+ = \frac{\frac{di_1^+}{dV_1^+}}{N^+ e \frac{C}{\epsilon}} \text{ for } V < V_o \quad (5.3)$$

have been used. The equation (5.2) is obtained from equation (2.11) with V_o as is given by equation (2.12), and equation (5.3) is derived from equation (2.10) and (5.2).

The results of positive ion densities and positive ion mobilities as a function of altitude for flight, made on January 11, 1974 at WSMR



(a)



(b)

Figure 23. Two Typical Current-Voltage Characteristics of the Gerdien Condenser at: (a) 62 km, (b) 39 km.

are given in Figures 24 and 25, respectively. Above 47 km two groups of positive ions are present; the heavier group is about an order of magnitude less mobile than the lighter group. Between about 38 and 47 km the positive ions with different densities and their mobility spectrum are represented by straight lines. Below about 38 km the applied sweep voltage is not high enough to saturate the Gerdien condenser, consequently; no data is given. A preliminary analysis of the strip chart data indicates that electrons have not been collected for the most of the flight, therefore, the negative ion densities and mobilities have not been calculated.

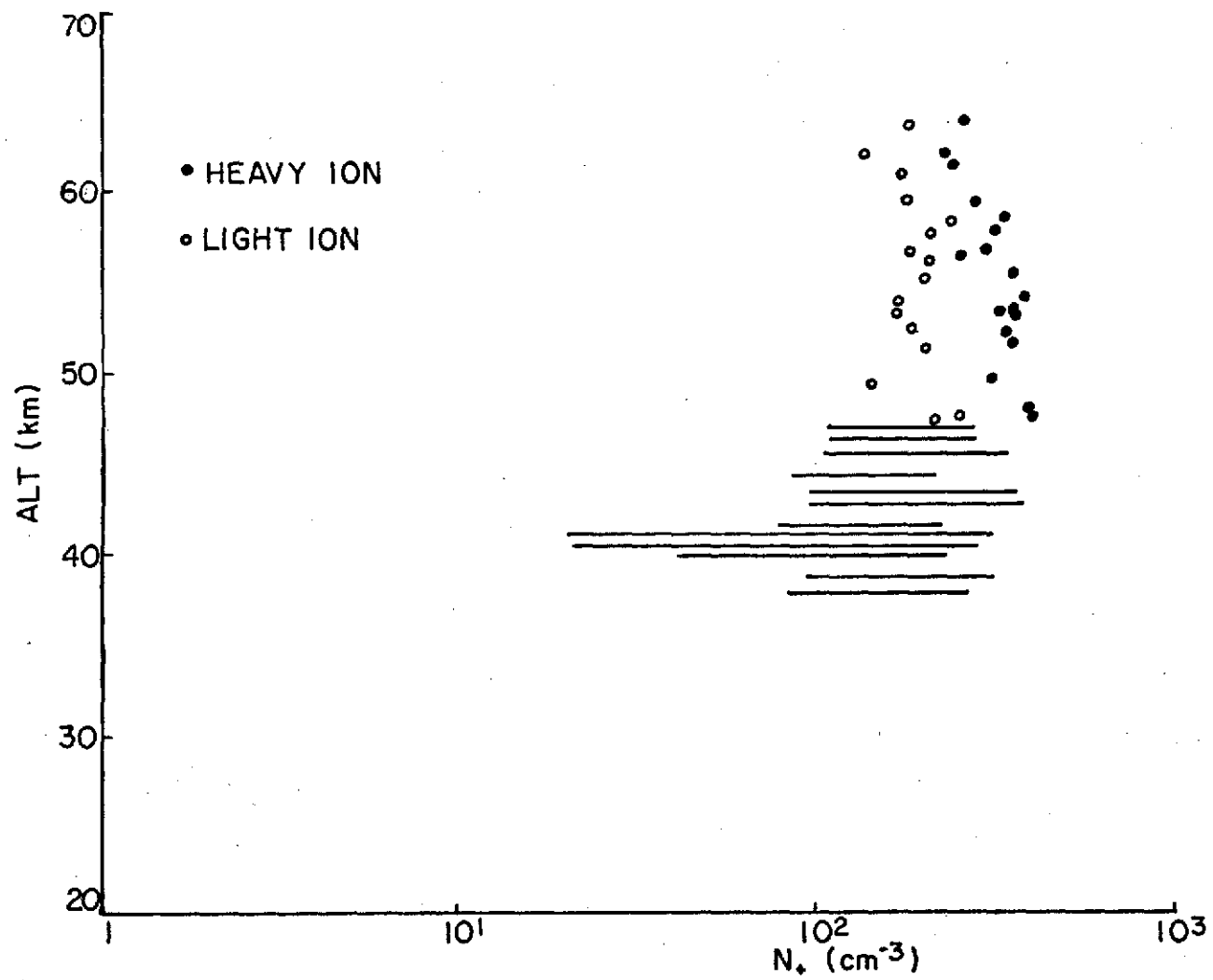


Figure 24. Positive Ion Density as a Function of Altitude.

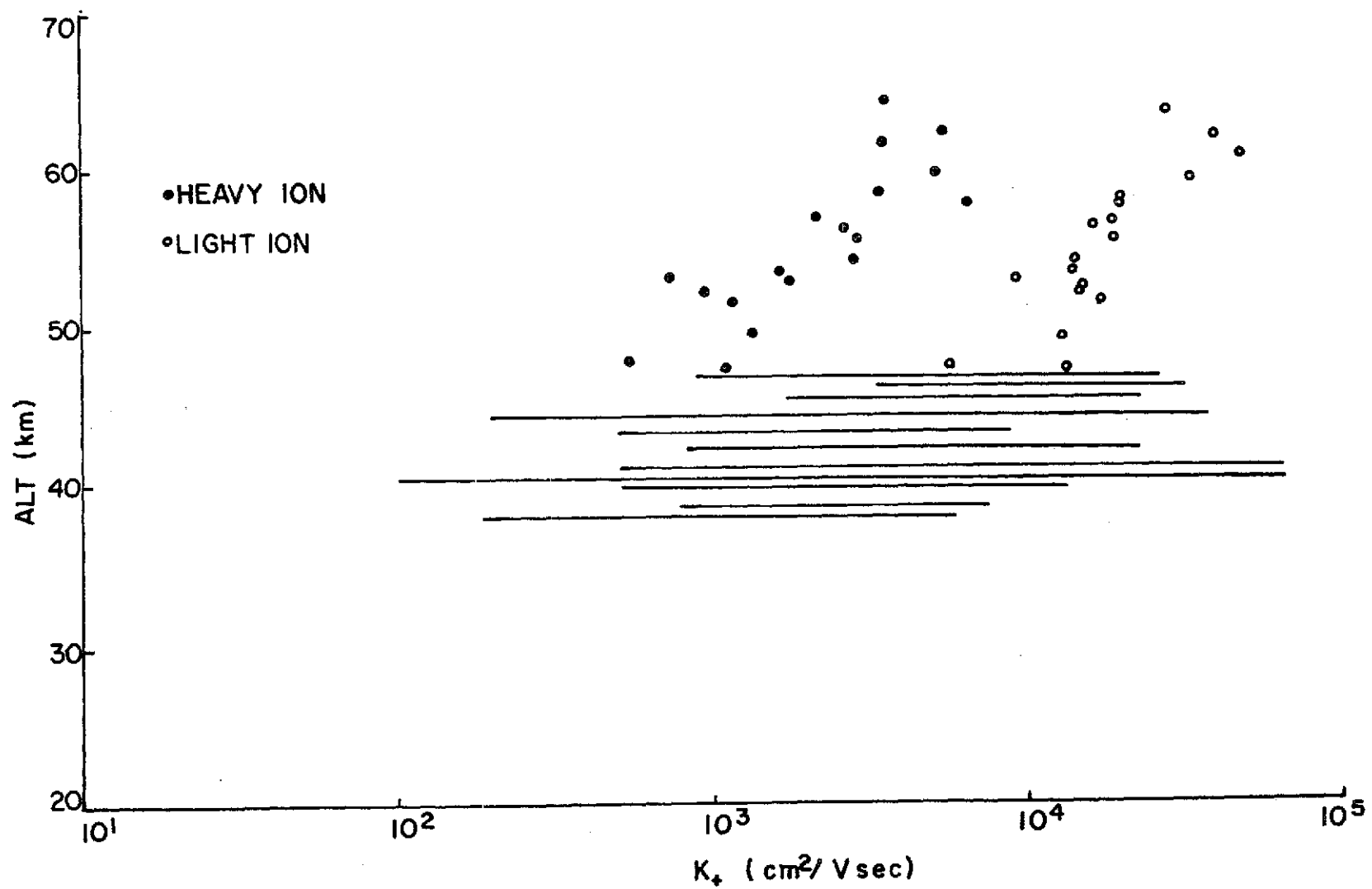


Figure 25. Positive Ion Mobility as a Function of Altitude.

CHAPTER VI

CONCLUSIONS

The absence of reliable D-region particle mobility data has resulted in the design of a simple Gerdien condenser (aspiration probe) system believed capable of accurately measuring ion density and mobility. The angle of attack problem associated with earlier instrument has been largely reduced by the use of an aerodynamically more stable device, a starute, manufactured by Space Data Corporation.

Because of nonlinearity in the differential equations involved, it has not been possible to determine the average velocity of air flow through the condenser theoretically, even in case of relatively simple incompressible laminar flow (Chapter IV). Therefore, the average velocity or the volume rate of air flow through the Gerdien condenser must be evaluated experimentally; it can be measured using a flow-meter (such as the one used by Rose and Widdel, 1972).

Experimental results of 11 January 1974 at WSMR (Figures 24 and 25) show the positive ion densities and mobilities between an altitude range of about 38 and 65 km. At lower altitude the applied sweep voltage was not high enough to saturate the condenser; it seems increase of positive peak of voltage waveform from +5 to +10 volts is sufficient to saturate the instrument having the descent velocity of this order (Figure 13). Electrons were not collected effectively in this experiment. A possible reason may be electrons having relatively high mobility were reflected before reaching the device.

REFERENCES

- Bird, R. B., W. E. Stewart, and E. N. Lightfoot, Transport Phenomena, Wiley and Sons, New York, 1960.
- Bourdeau, R. E., E. C. Whipple, and J. F. Clark, Analytical and experimental electrical conductivity between the stratosphere and ionosphere, J. Geophys. Res., 64, 1363-1370, 1959.
- Chesworth, E. T., The role of ice particulates in the electrification of the air in the mesosphere, Ph.D. Thesis in Physics, The Pennsylvania State University, 1974.
- Conley, T. D., Mesospheric positive ion concentration, mobility, and loss rates obtained from rocket-borne Gerdien condenser measurements, Radio Sci., 9, 575-592, 1974.
- Coyne, T. N. R. and J. S. Belrose, The diurnal and seasonal variation of electron densities in the mid-latitude D-region under quiet conditions, Radio Sci., 7, 163-174, 1972.
- Cuffin, B. N., A circular slot antenna for use on ionospheric probes, PSU-IRL-SCI-346, The Pennsylvania State University, 1965.
- Deeks, D. G., D-region electron distribution in middle latitudes deduced from the reflexion of long radio waves, Proc. Roy. Soc. London, A291, 413-437, 1966.
- Gerdien, H., Demonstration eines apparatuses Zur absoluten messung der electreschen leitfahigut der luft, Terr. Magn. Atmos. Elec., 10, 65-79, 1905.
- Goldstein, S., Modern Developments in Fluid Dynamics, Vol. 1, Oxford University Press, New York, 1938.
- Hale, L. C., L. C. Nickell, B. Kennedy, and T. A. Powell, Supersonic and subsonic measurements of mesospheric ionization, Radio Sci., 7, 89-91, 1972.
- Israel, H. and L. Schulz, The mobility-spectrum of atmospheric ions- Principles of measurements and results, Terr. Magn. Atmos. Elec., 38, 285-300, 1933.
- Jespersen, M., A. J. Kane, and B. Landmark, Electron and positive ion density measurements during conditions of auroral absorption, J. Atmos. Terr. Phys., 30, 1955-1963, 1968.
- Kelly, H. R., A note on the laminar boundary layer on a circular cylinder in axial incompressible flow, J. Aero. Sci., 21, 634, 1954.
- Kennard, E. H., Kinetic Theory of Gases, McGraw-Hill, New York, 1938.

- Knoll, M., J. Eichmeier, and R. W. Schou, Properties, measurement and bioclimatic action of "small" multimolecular atmospheric ions, Advances in Electronics and Electron Physics, edited by L. Marton, Academic Press, New York, 177-254, 1964.
- Kraakevik, J., The airborne measurement of atmospheric conductivity, J. Geophys. Res., 63, 161-169, 1958.
- Kroening, J. L., Ion-density measurements in the stratosphere, J. Geophys. Res., 65, 145-157, 1960.
- Lee, H. S. and A. J. Ferraro, Winter D-region electron concentration and collision frequency features obtained with high-power inter-action measurements, J. Geophys. Res., 74, 1184-1194, 1969.
- Liepmann, H. W. and A. Roshko, Elements of Gasdynamics, Wiley and Sons, New York, 1957.
- Loeb, L. B., Basic Processes of Gaseous Electronics, University of California Press, Berkeley and Los Angeles, 1961.
- Maris, H. B., The upper atmosphere, Terr. Magn., 33, 45-53, 1929.
- Nolan, P. J. and P. J. Kenney, A modified McClelland method for measuring ionic mobilities, J. Atmos. Terr. Phys., 2, 266-271, 1952.
- Paltridge, G. W., Experimental measurement of the small-ion density and electrical conductivity of the stratosphere, J. Geophys. Res., 70, 2751-2761, 1965.
- Pederson, A., Measurement of ion concentration in the D-region of the ionosphere with a Gerdien condenser rocket probe, FOA 3 Report A607, Research Institute of National Defense, Electronics Dept., Stockholm, 1963.
- Rose, G. and H. U. Widdel, Results of concentration and mobility measurements for positively and negatively charged particles taken between 85 and 22 km in sounding rocket experiments, Radio Sci., 7, 81-87, 1972.
- Sagalyn, R., The production and removal of small ions and charged nuclei over the Atlantic Ocean, in Recent Advances in Atmospheric Electricity, edited by L. G. Smith, Pergamon Press, London, 1958a.
- Shames, I. H., Mechanics of Fluids, McGraw-Hill, New York, 1962.
- Shmeer, H. and A. Hack, Z. Angew. Phys., 14, 398, 1962. Material from the source not available but quoted in secondary source (Knoll et al., 1964).
- Sonin, A. A., Theory of ion collection by a supersonic atmospheric sounding rocket, J. Geophys. Res., 72, 4547-4557, 1967.

Stergis, C. G., S. C. Coroniti, A. Nazarek, D. E. Kotas, D. W. Seymour, and J. V. Werme, Conductivity measurement in the stratosphere, J. Atmos. Terr. Phys., 6, 233-242, 1955.

Thrane, E. V., A. Haug, B. Bjelland, M. Anastassiades, and E. Tsagakis, Measurements of D-region electron densities during the international quiet sun years, J. Atmos. Terr. Phys., 30, 135-150, 1968.

Tsien, H. S., Superaerodynamics, mechanics of rarefied gases, J. Aero. Sci., 13, 653-664, 1946.

Wannier, G. H., Motion of gaseous ions in strong electric fields, Bell Syst. Tech. J., 32, 170-254, 1953.

Whipple, E. C., Jr., Electricity in the terrestrial atmosphere above the exchange layer, NASA Tech. Note D-2092, 1964.

Woessener, R. H., W. E. Cobb, and R. Gunn, Simultaneous measurement of the positive and negative light ion conductivities to 26 kilometers, J. Geophys. Res., 63, 171-180, 1958.

York, T. M., Private Communication, 1974.

APPENDIX A

COMPUTER PROGRAM

```
C      A SIMPLE PROGRAM TO CALCULATE DISPLACEMENT THICKNESS
C      IN 'GERDIEN CONDENSER'.
      A=3.7E-2
      B=7E-3
      ABS=1E-3
      WRITE(6,16)
      GO TO 20
20 READ(5,10,END=100)M,V,UO,D
10 FORMAT(12,E10.3,2X,F10.1,5X,E8.2)
      UC=UO
      GO TO 14
14 P=SWRT(V*D/UC)
      DELO=3.442/3.*P
C      'DELO' IS THE AVERAGE DIS. THICKNESS IN OUTER CYLINDER, AFLAT PLATE
C      APPROX. HAS BEEN ASSUMED.
      R=4./B*P
      DELI=1.721*P*(2./3.-.102*R+.292/5.*R**2)
C      'DELI' IS THE AVERAGE DIS. THICKNESS ON INNER CYLINDER, BASED
C      ON KELLY'S RESULT.
      F=3.14*(A**2-B**2)*UO
      FDEL=3.14*((A-DELO)**2-(B+DELI)**2)*UC
C      F AND FDEL ARE FLUXES AT ENTRANCE AND ACROSS SECTION, WHERE
C      DIS. THICKNESS HAS BEEN TAKEN INTO ACCOUNT, RESPECTIVELY.
      IF(FDEL.GT.F) GO TO 12
      UC=UC+ABS
C      A ITERATIVE METHOD IS USED, UC IS INCREASED BY AN INCREMENT
C      OF .001 UNTIL FDEL=F(CONSTANCY OF FLUXES).
      GO TO 14
12 WRITE(6,18)M,DELI,DELO,UC,F,FDEL
18 FORMAT(15X,12,2(8X,E10.4),10X,F6.2,2(9X,E10.4))
      GO TO 20
16 FORMAT(13X,'ALT.:',13X,'DELI:',13X,'DELO:',6X,'CORE VEL.:',5X,
1'FLUX AT ENT.:',8X,'CORE FLUX: '//)
100 STOP
      END
```

Farrokhi, Hashem, Design of a Simple Gerdien Condenser for Ionospheric D-Region Charged Particle Density and Mobility Measurements, The Ionosphere Research Laboratory, Electrical Engineering East, University Park, Pennsylvania, 16802, 1975.

The theory of a Gerdien Condenser operating in a collision-controlled medium is reviewed. Design and electronics of a Gerdien condenser probe suitable for flying on the Arcas rocket is presented. Aerodynamics properties of the instrument in continuous flow are discussed. The method of data reduction and experimental results of one successful flight at White Sands Missile Range (WSMR), New Mexico on 11 January 1974 is reported. The result of this investigation shows: positive ions in two relatively distinct mobility groups between 47 and 65 km and a more continuous distribution of mobilities between 38 and 47 km.

PSU-IRL-SCI-433

Classification Numbers:

- 1.5.1 D-Region
- 3.2.2 Rocket-Satellite Techniques and Measurements

Farrokhi, Hashem, Design of a Simple Gerdien Condenser for Ionospheric D-Region Charged Particle Density and Mobility Measurements, The Ionosphere Research Laboratory, Electrical Engineering East, University Park, Pennsylvania, 16802, 1975.

The theory of a Gerdien Condenser operating in a collision-controlled medium is reviewed. Design and electronics of a Gerdien condenser probe suitable for flying on the Arcas rocket is presented. Aerodynamics properties of the instrument in continuous flow are discussed. The method of data reduction and experimental results of one successful flight at White Sands Missile Range (WSMR), New Mexico on 11 January 1974 is reported. The result of this investigation shows: positive ions in two relatively distinct mobility groups between 47 and 65 km and a more continuous distribution of mobilities between 38 and 47 km.

PSU-IRL-SCI-433

Classification Numbers:

- 1.5.1 D-Region
- 3.2.2 Rocket-Satellite Techniques and Measurements

Farrokhi, Hashem, Design of a Simple Gerdien Condenser for Ionospheric D-Region Charged Particle Density and Mobility Measurements, The Ionosphere Research Laboratory, Electrical Engineering East, University Park, Pennsylvania, 16802, 1975.

The theory of a Gerdien Condenser operating in a collision-controlled medium is reviewed. Design and electronics of a Gerdien condenser probe suitable for flying on the Arcas rocket is presented. Aerodynamics properties of the instrument in continuous flow are discussed. The method of data reduction and experimental results of one successful flight at White Sands Missile Range (WSMR), New Mexico on 11 January 1974 is reported. The result of this investigation shows: positive ions in two relatively distinct mobility groups between 47 and 65 km and a more continuous distribution of mobilities between 38 and 47 km.

PSU-IRL-SCI-433

Classification Numbers:

- 1.5.1 D-Region
- 3.2.2 Rocket-Satellite Techniques and Measurements